OXFORD GENETICS

GENETICS, 2022, 220(1), iyab199
https://doi.org/10.1093/genetics/iyab199
Advance Access Publication Date: 15 November 2021
Investigation

Single nucleotide substitutions effectively block Cas9 and allow for scarless genome editing in *Caenorhabditis elegans*

Jeffrey C. Medley, Shilpa Hebbar, Joel T. Sydzyik, and Anna Y. Zinovyeva *

Division of Biology, Kansas State University, Manhattan, KS 66502, USA

*Corresponding author: Division of Biology, Kansas State University, 28 Ackert Hall, Manhattan, KS 66506, USA. Email: zinovyeva@ksu.edu

Abstract

In *Caenorhabditis elegans*, germline injection of Cas9 complexes is reliably used to achieve genome editing through homology-directed repair of Cas9-generated DNA breaks. To prevent Cas9 from targeting repaired DNA, additional blocking mutations are often incorporated into homologous repair templates. Cas9 can be blocked either by mutating the PAM sequence that is essential for Cas9 activity or by mutating the guide sequence that targets Cas9 to a specific genomic location. However, it is unclear how many nucleotides within the guide sequence should be mutated, since Cas9 can recognize "off-target" sequences that are imperfectly paired to its guide. In this study, we examined whether single-nucleotide substitutions within the guide sequence are sufficient to block Cas9 and allow for efficient genome editing. We show that a single mismatch within the guide sequence effectively blocks Cas9 and allows for recovery of edited animals. Surprisingly, we found that a low rate of edited animals can be recovered without introducing any blocking mutations, suggesting a temporal block to Cas9 activity in *C. elegans*. Furthermore, we show that the maternal genome of hermaphrodite animals is preferentially edited over the paternal genome. We demonstrate that maternally provided haplotypes can be selected using balancer chromosomes and propose a method of mutant isolation that greatly reduces screening efforts postinjection. Collectively, our findings expand the repertoire of genome editing strategies in *C. elegans* and demonstrate that extraneous blocking mutations are not required to recover edited animals when the desired mutation is located within the guide sequence.

Keywords: genome editing; CRISPR; Cas9; blocking; scarless; miRNA; noncoding RNA; *C. elegans*; *let-7*

Introduction

The CRISPR/Cas9 system has become increasingly used to facilitate genome editing in numerous organisms (Ma and Liu 2015; Shrock and Güell 2017; Ma *et al.* 2018). Cas9 (CRISPR-associated protein 9) is a programmable endonuclease whose specificity is governed by a guide RNA that has sequence complementarity to a specific genomic location (Jinek *et al.* 2012). The guide RNA comprises two molecules: the CRISPR RNA (crRNA) that contains a 20-nucleotide guide sequence and a trans-acting CRISPR RNA (tracrRNA) that forms a duplex with the crRNA and bridges the guide RNA to Cas9 (Deltcheva *et al.* 2011; Jinek *et al.* 2012). A protospacer-adjacent motif (PAM) sequence is located immediately downstream of the RNA guide-complementary genomic sequence and is required for Cas9 to initiate a double-stranded DNA break. In the case of *Streptococcus pyogenes* Cas9, commonly used for genome editing, the nucleotide PAM sequence is NGG, where N is any nucleotide (Mojica *et al.* 2009; Marraffini and Sontheimer 2010; Jinek *et al.* 2012; Sashital *et al.* 2012). Once a double-stranded DNA break is created, the break is typically repaired through one of two mechanisms: nonhomologous end joining (NHEJ) or homology-directed repair (HDR) (Ceccaldi *et al.* 2016; Li and Xu 2016; Scully *et al.* 2019; Han and Huang 2020; Yang *et al.* 2020). In NHEJ, the broken DNA is repaired through direct ligation of the broken DNA ends. However, this process is error prone as the ligation often requires processing of the broken ends, resulting in additions or deletions of nucleotide bases at the break site (Chang *et al.* 2017; Zhao *et al.* 2020). Conversely, HDR uses a donor DNA molecule that has homology surrounding the break site as a template to precisely repair the broken DNA (Haber 2018; Ranjha *et al.* 2018; Sun *et al.* 2020). Therefore, HDR has been widely adapted to repair Cas9-generated DNA breaks to introduce precise genome edits in a broad range of organisms. Donor repair templates can be exogenously provided as single-stranded oligodeoxynucleotides (ssODN) or double-stranded DNA (dsDNA) molecules for the purpose of genome editing (Cong *et al.* 2013; Zhao *et al.* 2014; Paquet *et al.* 2016; Yoshimi *et al.* 2016; Gallagher *et al.* 2020). During CRISPR/Cas9-mediated genome editing, the process of HDR using an ssODN repair template is referred to as single-stranded template repair (SSTR), and results in higher genome editing efficiencies than HDR pathways that use dsDNA repair templates (Katic *et al.* 2015; Dokshin *et al.* 2018; Richardson *et al.* 2018; Liu *et al.* 2019; Okamoto *et al.* 2019; Gallagher *et al.* 2020; Gallagher and Haber 2021).

Received: September 13, 2021. **Accepted:** October 28, 2021

Once a Cas9-generated DNA break is repaired through SSTR, Cas9 must be prevented from continuing to target the repaired DNA. To accomplish this, additional blocking mutations are often incorporated into homologous repair templates, disrupting the ability of Cas9 to target the repaired sequence. As the PAM is absolutely required for Cas9 activity (Mojica *et al.* 2009; Marraffini and Sontheimer 2010; Jinek *et al.* 2012; Sashital *et al.* 2012), the most straightforward way to block Cas9 is to introduce silent mutations into the PAM. Alternatively, Cas9 can be blocked by introducing mutations into the guide sequence, which targets Cas9 to a specific genomic location (Deltcheva *et al.* 2011; Jinek *et al.* 2012). However, studies in human cells have shown that Cas9 is capable of recognizing off-target sequences that are imperfectly paired to its guide RNA (Jinek *et al.* 2012; Pattanayak *et al.* 2013; Jiang and Doudna 2015). Mismatches near the 3′ end of the guide RNA appear to be more effective at blocking Cas9 compared to mismatches toward the 5′ end of the guide RNA (Jinek *et al.* 2012; Cong *et al.* 2013; Fu *et al.* 2013; Hsu *et al.* 2013; Mali *et al.* 2013; Pattanayak *et al.* 2013; Zhang *et al.* 2015). Increasing the number of mismatches generally leads to increased blocking efficacy (Jinek *et al.* 2012; Cong *et al.* 2013; Fu *et al.* 2013; Hsu *et al.* 2013; Mali *et al.* 2013; Pattanayak *et al.* 2013; Zhang *et al.* 2015). Nevertheless, Cas9 has been reported to cleave DNA sequences containing up to five mismatches to certain guide RNAs (Hsu *et al.* 2013), although three mismatches effectively block Cas9 for most guide RNAs (Fu *et al.* 2013; Hsu *et al.* 2013; Mali *et al.* 2013). Therefore, it remains unclear how many nucleotides should be mismatched and where the mismatches should be located within the guide sequence to effectively block Cas9 for genome editing *in vivo*.

In the nematode *Caenorhabditis elegans*, injection of Cas9 ribonucleotide protein (RNP) complexes and ssODN repair templates into the germline of hermaphrodite animals has been reliably used to facilitate heritable genome editing (Paix *et al.* 2015, 2017; Farboud *et al.* 2019). However, certain types of genome edits remain challenging to design due to the need to block Cas9 from targeting the repaired DNA. Protein coding sequences are highly amenable for genome editing experiments, as codon redundancy frequently allows silent blocking mutations to be introduced without changing the amino acid identity. However, genome editing of regulatory and nonprotein coding portions of the genome remain a challenge. It is often difficult to predict how extraneous blocking mutations may affect the function of noncoding regulatory sequences such as noncoding RNAs, untranslated regions, and other regulatory elements. Extraneous blocking mutations can be avoided when the intended edit also alters a PAM site and eliminates Cas9 ability to recut a repaired genome site. In such cases, genome editing is performed in a "scarless" fashion. However, the dinucleotide GG of the PAM sequence (NGG) is only expected to occur, on average, every 16 bases and must overlap with the desired edit to generate a scarless edit. This frequency is likely reduced in noncoding regions that are often AT-rich. It has been suggested that single nucleotide substitutions located within three nucleotides of the PAM are sufficient to allow for genome editing in *C. elegans* (Paix *et al.* 2017; Farboud *et al.* 2019). This is of particular interest for scarless genome editing, as non-PAM mutations could block Cas9 and thereby bypass the need for additional blocking mutations. We reasoned that single nucleotide substitutions beyond the three PAM-adjacent nucleotides, located in the guide-binding region could effectively block Cas9, further facilitating scarless genome editing of noncoding sequences. Toward this end, we have performed a systematic analysis of the blocking efficacy of single nucleotide mismatches throughout the guide sequence in *C. elegans*. We demonstrate that single nucleotide substitutions throughout the guide-binding sequence are sufficient to block Cas9 and allow for effective recovery of edited animals. Furthermore, we were able to recover heritable genome edited strains without introducing any blocking mutations, suggesting that a temporal block to Cas9 activity limits the ability of Cas9 to target repaired DNA. We also show that editing of the maternal genome of self-fertile hermaphrodite animals occurs at much greater frequency compared to editing of the paternal genome. Finally, we propose a new method of mutant isolation that selects for maternally provided haplotypes and greatly reduces screening efforts postinjection. As a proof-of-principle, we use this method to generate otherwise scarless genome edits in the *let-7* microRNA. Our collective findings expand the repertoire of possible genome edits in *C. elegans* and will facilitate scarless editing of noncoding sequences.

Materials and methods

Caenorhabditis elegans strains and genetics

All *C. elegans* strains were derived from the wild-type N2 strain and maintained at 20°C unless otherwise noted. Strains were grown under standard conditions using nematode growth medium (NGM) plates seeded with *Escherichia coli* OP50 (Brenner 1974). A full list of strains used in this study is provided in Supplementary Table S1.

For experiments examining maternal *vs* paternal editing, matings were performed by adding several wild-type males to a plate containing L4-staged, *tra-2* mutant hermaphrodite animals generated in this study. For *let-7* genome editing experiments, several males containing the *tmc24* balancer were mated to L4-staged, wild-type hermaphrodite animals. Animals were allowed to mate 16–24 h prior to injection. Successful mating was verified by genotyping F1 animals through *RsaI* digestion to confirm *tra-2* heterozygosity, or presence of pharyngeal Venus to confirm presence of the *tmc24* balancer.

CRISPR/Cas9 genome editing

Commercially available *S. pyogenes* Cas9 (IDT, Alt-R® S.p. Cas9 Nuclease V3) was injected at a final concentration of 2.65 μM and was included in all injection mixes. All injection mixtures also contained 200 μM KCI and 7.5 μM HEPES [pH 7.4]. Each injection mix contained one or two crRNAs targeting *dpy-10* (5 μM), *tra-2* (50 μM) or *let-7* (50 μM), and equimolar tracrRNA was included (5, 50, or 55 μM). Single-stranded DNA oligonucleotides for *dpy-10* (3 μM), *tra-2* (6 μM), and *let-7* (6 μM) were used to facilitate HDR (Supplementary Table S2).

To generate nondumpy genome edits at the *tra-2* locus, which we used to examine how effectively single nucleotide substitutions blocked Cas9, we replaced *dpy-10* coconversion with the Pmyo-2::mCherry coinjection marker (5 ng/μl). The Pmyo2::mCherry coinjection marker was included to mark broods that were successfully injected and to enrich for genome-edits as previously described (Prior *et al.* 2017). A full list of oligonucleotides (IDT) used in this study is provided in Supplementary Table S2.

Screening and genotyping

For experiments testing the efficacy of *tra-2* editing, we blindly sequenced (*i.e.*, without *RsaI* digestion) the F2 generation Dumpy and nondumpy animals originating from each F1 Roller animal. F1 Rollers were picked from jackpot broods (Paix *et al.* 2015) that were defined as having >20 F1 Rollers from a single P0 injected animal. F1 rollers that did not produce Dumpy, Roller and

nondumpy progeny were excluded from our analysis. The *tra-2* genomic locus was PCR amplified using the primers 5′-CTGCTAAAGGTTAGTTGTT-3′ and 5′-ATAATGTATTCTTCATTGTTCG-3′ and sequenced using the primer 5′-ATTTTAGGAATAATTGGAGCC-3′. All *Rsa*I digestions were performed at 37°C for at least 1 h. A *Rsa*I-positive control was included on all gels used for quantification to confirm successful *Rsa*I digestion occurred.

To examine genome editing of *let-7*, we singled F1 generation Roller animals from jackpot broods that showed pharyngeal Venus signal that indicated successful mating to the tmc24 balancer preinjection. We then blindly sequenced F2 generation animals lacking pharyngeal Venus that were therefore homozygous for the maternally provided X-chromosome haplotype. The *let-7* genomic locus was PCR amplified using the primers 5′-GTTTGCGTATGTGTATGTAG-3′ and 5′-TCCCCTGAAAATAAAACATGA-3′ and sequenced using the primer 5′-TATTCTAGATGAGTAGCCCA-3′. All genome edits were verified through Sanger sequencing.

Statistical analysis

All *P*-values were calculated using two-tailed *t*-tests assuming equal variance. All statistics are presented as mean ± 1 standard deviation.

Results

Coconversion of tightly linked genes to test genome editing efficiency

In *C. elegans*, standard genome-editing practices involve injection of Cas9, guide RNAs and homologous repair templates into the germline of self-fertile hermaphrodite adult animals (Xu 2015; Chen *et al.* 2016; Dickinson and Goldstein 2016; Farboud 2017; Iyer *et al.* 2018; Kim and Colaiácovo 2019; Nance and Frøkjær-Jensen 2019; Ghanta and Mello 2020). Due to the syncytial nature of the distal gonad, a single injection can be distributed among numerous germ cells (Evans 2006; Kadandale *et al.* 2008). Although injection of Cas9 into the distal germline is expected to affect the genomes of maternal oocytes, homozygously edited animals can be recovered from the F1 generation postinjection, suggesting that editing of both maternal and paternal germ cells can occur from a single injection (Friedland *et al.* 2013; Kim *et al.* 2014; Zhao *et al.* 2014; Paix *et al.* 2015; Wang *et al.* 2018). In addition, PCR amplification of heterozygous animals may not amplify large deletions if the deletions affect primer binding sites (Katic and Großhans 2013; Kim *et al.* 2014; Dokshin *et al.* 2018; Wang *et al.* 2018), further complicating quantification of genome editing rates by providing an inaccurate picture of editing nature (HDR or indel) and frequency. Overall, edited F1 animals can carry maternal genome edits, paternal genome edits, or both. Unless both maternal and paternal haplotypes can be analyzed separately, it can be difficult to determine whether one or two independent genome editing events may have occurred, complicating quantification of genome editing rates.

Therefore, we first aimed to develop a new method for quantifying genome editing rates that would allow separate analysis of each parental haplotype (Figure 1A). We used a coediting (co-CRISPR) approach, using two tightly linked genes that were simultaneously targeted using two different guide RNAs (Figure 1A). An advantage of coediting is that the editing of one locus ensures that Cas9 was active and available to target the second locus, which can at least partially normalize injection efficiencies across different injections (Kim *et al.* 2014; Paix *et al.* 2015). We chose to edit the *tra-2* gene, which is located on chromosome II, 0.16 map units away from the commonly used co-CRISPR gene *dpy-10*. The *dpy-10(cn64)* variation results in a semi-dominant phenotype that is easily visualized on a stereomicroscope (Arribere *et al.* 2014; Paix *et al.* 2015). Animals homozygous for the *dpy-10(cn64)* mutation have a dumpy phenotype marked by a reduced body length whereas heterozygous animals have a normal body length but display an abnormal rolling behavior (Figure 1A, Arribere *et al.* 2014; Paix *et al.* 2015).

Due to their close proximity, meiotic recombination between *tra-2* and *dpy-10* is only expected in 1/625 haplotypes. Therefore, the haplotype arrangement of *tra-2* and *dpy-10* alleles will be stably maintained across generations (Figure 1A). As F1 generation roller animals contain a single *dpy-10(cn64)*-marked (Dpy-marked) chromosome and one chromosome that is not Dpy-marked, we were able to distinguish the two parental haplotypes and determine whether either or both haplotypes carried an edited allele of *tra-2* (Figure 1A). Segregation of dumpy and nondumpy animals in the F2 generation homozygoses for each F1 generation haplotype, which allowed us to definitively determine whether one or two genome editing events had taken place in the F1 generation by sequencing the *tra-2* genomic locus (Figure 1A).

Single nucleotide blocking mutations in the guide-binding region allow for effective genome editing

To determine whether single nucleotide substitutions in the guide-binding region effectively block Cas9 and allow for recovery of genome-edited animals, we designed a series of blocking mutations within a guide-binding region located in the 5′ UTR of *tra-2* (Figure 2A). Because previous reports have suggested that substitutions proximal to the 3′ end of the guide are more effective at blocking Cas9 (Jinek *et al.* 2012; Cong *et al.* 2013; Fu *et al.* 2013; Hsu *et al.* 2013; Mali *et al.* 2013; Pattanayak *et al.* 2013; Zhang *et al.* 2015), we introduced substitutions every three nucleotides to test the positional effects of single nucleotide blocking mutations (Figure 2A). We named each mutation according to its position ("P") relative to the 3′ end of the guide sequence (Figure 2A). For example, we refer to the mutation affecting the second nucleotide from the 3′ end of the guide sequence as "P2" and the mutation affecting the twentieth nucleotide from the 3′ end as "P20" (Figure 2A). As a control, we designed a mutation within the PAM domain, which is expected to completely block Cas9 activity (Mojica *et al.* 2009; Marraffini and Sontheimer 2010; Jinek *et al.* 2012; Sashital *et al.* 2012). Each of the repair templates were designed to also include a nonblocking, single nucleotide substitution downstream of the PAM sequence that introduces an *Rsa*I restriction enzyme cutting site (Figure 2A). As an additional control, we designed a repair template that only included the *Rsa*I cutting site, which should not block Cas9 activity. This repair template would therefore not be expected to allow for HDR editing since Cas9 should continue targeting the repaired DNA.

We performed co-CRISPR of *dpy-10* and *tra-2* for each of the blocking conditions that we designed (Figure 2A). We used ssODN repair templates, which themselves are not subject to Cas9 cleavage and effectively promote genome editing when injected alongside preassembled Cas9 RNP complexes in *C. elegans* (Paix *et al.* 2015). Following injection, we singled F1 generation roller animals from "jackpot" broods containing the highest percentage of F1 generation *dpy-10*-edited animals (Paix *et al.* 2015). As rollers are heterozygous for the *dpy-10(cn64)* variation, F2 progeny are a mixture of homozygous dumpy animals, heterozygous roller animals, and homozygous nondumpy animals (Figure 1). Because *tra-2* and *dpy-10* are genetically linked, F2 generation dumpy and

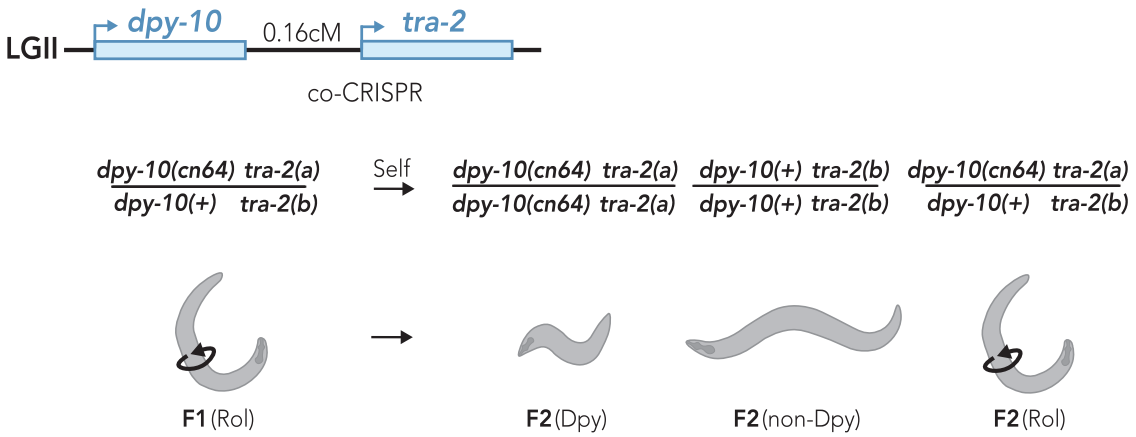

Figure 1 Strategy for coconversion of *dpy-10* and *tra-2* to quantify haploid genome editing efficiency. *dpy-10* and *tra-2* are located 0.16 map units apart on LGII and do not undergo independent assortment (~1/625 meiotic recombination frequency). The *dpy-10(cn64)* allele produces a semi-dominant, physical phenotype where heterozygous animals have a rolling phenotype and homozygous animals have a dumpy phenotype. Following co-CRISPR of *dpy-10* and *tra-2*, one haplotype of F1 rollers has an unknown allele of *tra-2* ("*tra-2(a)*") linked to the *dpy-10(cn64)* variation and a second haplotype where an unknown *tra-2* allele ("*tra-2(b)*") is linked to a wild-type allele of *dpy-10*. Following self-fertilization of F1 hermaphrodite rollers, F2 generation dumpy animals are expected to be homozygous for the *tra-2(a)* allele whereas nondumpy animals should be homozygous for the *tra-2(b)* allele.

nondumpy animals will each be homozygous for different alleles of *tra-2* (Figure 1). We then sequenced the *tra-2* genomic locus of the F2 animals to determine whether a single haplotype or both haplotypes had been edited. We scored the frequency of HDR editing and the frequencies of insertion or deletion (indel) mutations (Figure 2, B and C, Supplementary Table S3). In some cases, we observed alleles containing both indel mutations and HDR edits, which could result if Cas9 recuts an HDR-edited allele thereby preventing HDR. Because accurate HDR was not achieved, we classified alleles containing both indels and HDR edits as indels and not HDR-edited. We also quantified the number of animals that did not show any apparent editing of *tra-2* (unedited), which could represent alleles that were never targeted by Cas9 or alleles that were targeted by Cas9 but repaired back to the wild-type genomic sequence without incorporating any of the designed edits (Figure 2, B and C, Supplementary Table S3). We defined HDR-edited animals as any animal that incorporated any of the designed mutations, regardless of whether partial or complete repair had occurred. As the *tra-2* guide RNA targets the 5′ UTR of *tra-2*, relatively small indel mutations might lead to loss of *tra-2* function. Loss of *tra-2* is not lethal but results in masculinization of hermaphrodite animals (Hodgkin and Brenner 1977; Doniach 1986), which allowed us to recover deleterious mutations such as indels.

In F2 generation dumpy animals, we observed nearly complete HDR editing of *tra-2* when the PAM was mutated (95.4% HDR-edited, Figure 2B, Supplementary Table S3), which is consistent with PAM mutations blocking Cas9 activity (Mojica *et al.* 2009; Marraffini and Sontheimer 2010; Jinek *et al.* 2012; Sashital *et al.* 2012). We observed similarly high HDR-editing rates in F2 generation dumpy animals when the PAM was mutated alongside an additional single nucleotide mismatch in the guide-binding region such as P2+PAM (93.8% HDR-edited), P11+PAM (88.6% HDR-edited) or P20+PAM (89.5% HDR-edited, Figure 2B, Supplementary Table S3). Although the efficiency was slightly reduced compared to the PAM blocking conditions, we found that the P2 (80.0% HDR-edited), P5 (75.8% HDR-edited), P8 (67.6% HDR-edited), P11 (75.7% HDR-edited), P14 (59.1% HDR-edited), P17 (54.8% HDR-edited), and P20 (66.6% HDR-edited) single nucleotide guide substitutions allowed for effective HDR editing in F2 generation dumpy animals (Figure 2B, Supplementary Table S3). While we used *dpy-10* coconversion to at least partially normalize injection efficiencies (Kim *et al.* 2014; Paix *et al.* 2015), we cannot rule out the possibility that small differences in editing efficiencies observed under different blocking conditions could result from variation of injection efficiencies across each individual injection. Nevertheless, the position of the single nucleotide substitutions within the guide-binding region may influence the frequency of recovering HDR-edited animals, as substitutions closer to the 3′ end of the guide sequence tended to be more effective compared to substitutions near the 5′ end of the guide sequence (Figure 2B, Supplementary Table S3). For example, the P2 (80.0% HDR-edited), P5 (75.8% HDR-edited), and P8 (67.6% HDR-edited) substitutions located within the 3′ half of the guide sequence averaged significantly higher HDR-editing rates (74.5 ± 6.3% average HDR-edited) compared to the P14 (59.1% HDR-edited), P17 (54.8% HDR-edited), and P20 (66.6% HDR-edited) substitutions that are located in the 5′ half of the guide sequence (60.2% average HDR-edited, $P < 0.05$). This positional effect of guide substitutions was not surprising given that previous studies have demonstrated that mismatches near the 3′ end of the guide sequence are more effective at blocking Cas9 than mismatches near the 5′ end of the guide sequence (Jinek *et al.* 2012; Cong *et al.* 2013; Fu *et al.* 2013; Hsu *et al.* 2013; Mali *et al.* 2013; Pattanayak *et al.* 2013; Zhang *et al.* 2015).

Interestingly, for all blocking conditions examined, we noticed a substantial reduction in HDR editing efficiency of the *tra-2* locus in F2 generation nondumpy animals (Figure 2C, Supplementary Table S3) compared to their dumpy siblings (Figure 2B, Supplementary Table S3). For example, whereas the PAM blocking condition resulted in very high HDR-editing rates in F2 generation dumpy animals (95.4% HDR-edited, Figure 2B, Supplementary Table S3), the rate of HDR editing was much lower in their nondumpy siblings (6.8% HDR-edited, Figure 2C, Supplementary Table S3). Although all single nucleotide substitutions in the guide-binding region had lower HDR editing rates in F2 generation nondumpy animals compared to dumpy animals, we did not observe a strong correlation between the position of substitutions within the guide sequence and the efficiency of HDR editing for nondumpy animals (Figure 2C, Supplementary Table S3), which is in contrast to the positional effects that we observed in their dumpy siblings (Figure 2B, Supplementary Table S3). While the substitutions in the 3′ half of the guide sequence (P2, P5, and P8) resulted in recovery of more HDR-edited animals than substitutions in the 5′ half of the guide

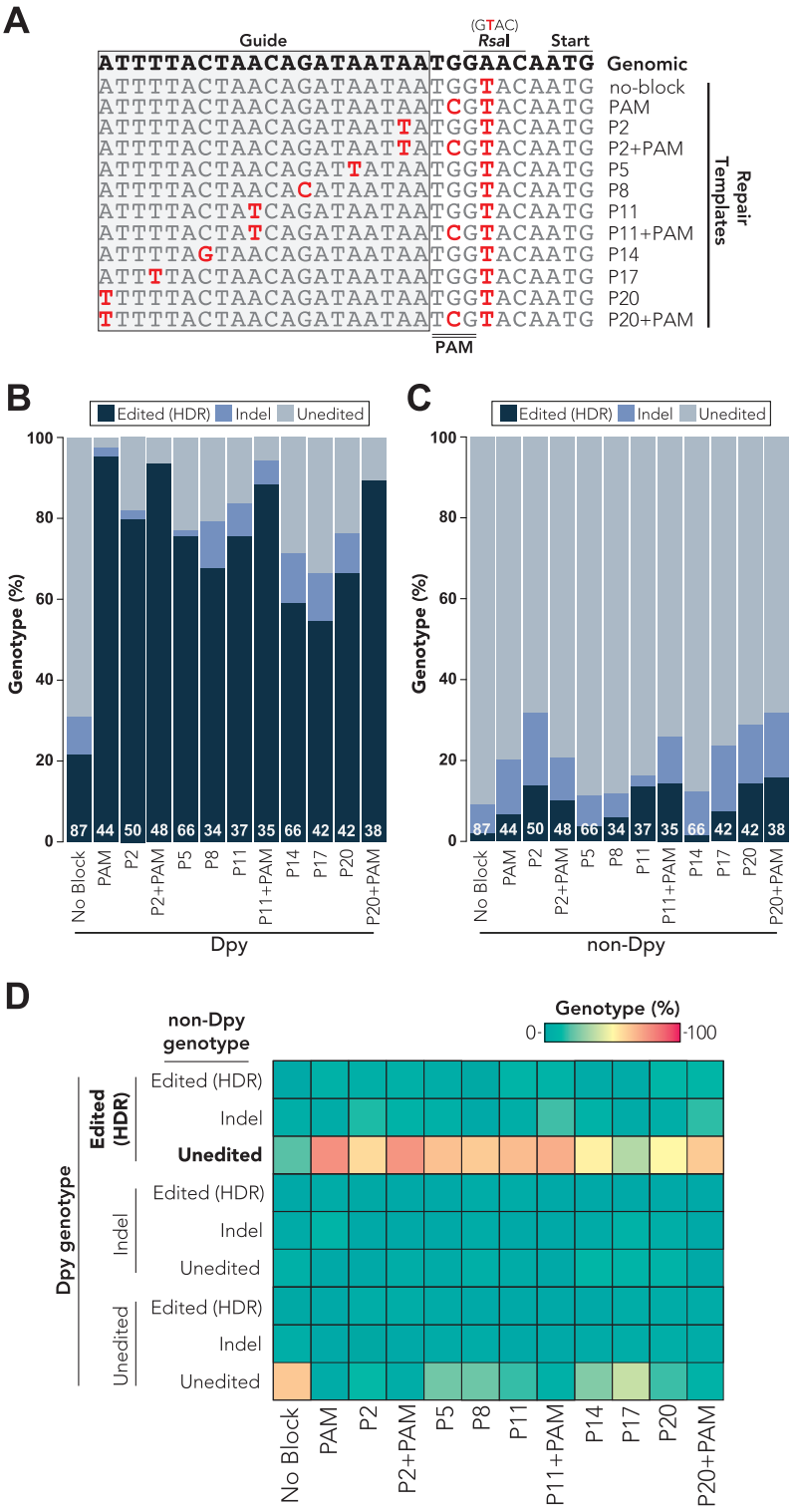

Figure 2 Single nucleotide mismatches in the guide RNA sequence allow for recovery of HDR-edited animals. (A) Partial alignment of *tra-2* repair templates used for genome editing experiments. See Supplementary Table S2 for full-length sequences of all repair templates. The wild-type genomic sequence is shown on the top line in bold text. Changes to the genomic sequence are indicated in red text. "P" refers to position on the guide sequence (gray-shaded box) counting from the 3′ end of the guide. The PAM sequence is indicated by a double bar (below). (B,C) Percent *tra-2* genotypes observed for F2 generation dumpy (B) or nondumpy (C) animals singled from F1 generation rollers. Edited (HDR) events were defined as partial or complete incorporation of genome edits engineered into single-stranded DNA repair templates. Indels were defined as any insertion or deletion mutation, regardless of whether editing through HDR may have also occurred. Unedited animals had no apparent changes compared to the wild-type *tra-2* genomic sequence. White text at the bottom of each stacked bar indicates the number (*n*) of animals that were sequenced. (D) Paired analysis of F2 generation dumpy and nondumpy genotypes from a single F1 generation roller. Heatmap indicates the % genotypes observed for each different blocking condition, where the sum of each column adds to 100% genotypes. Indel mutations were defined as any insertion or deletion mutation, regardless of whether editing through HDR may have also occurred. The most frequent observation (edited dumpy animals with unedited nondumpy siblings) is bolded. All results were determined through Sanger sequencing of singled F2 generation dumpy or nondumpy animals.

sequence (P14, P17, and P20) in dumpy animals (Figure 2B, Supplementary Table S3), the same substitutions in the 3′ half of the guide sequence resulted in a similar HDR-editing rate (8.67 ± 4.62% average HDR-edited) as substitutions in the 5′ half of the guide sequence (7.67 ± 6.41% average HDR-edited, $P = 0.83$) for the F2 generation nondumpy siblings (Figure 2C, Supplementary Table S3). Importantly, we were able to recover HDR-edited animals for all blocking mutations that we tested in F2 generation dumpy and nondumpy animals, showing that single nucleotide guide substitutions are sufficient to allow for effective HDR-editing in *C. elegans* and can be used as an alternative to PAM mutations when silently mutating the PAM is not possible.

We also quantified the frequency of indel mutations that occurred in the *tra-2* locus for each blocking condition that we tested (Figure 2, B and C, Supplementary Table S3). Because indels often result from NHEJ repair pathways, the presence of indels might suggest that NHEJ had been favored over HDR, which might be expected under conditions where Cas9 was not completely blocked. Consistent with this idea, we observed low indel rates in F2 generation dumpy animals when the PAM was mutated (2.3% indels) or when the PAM was mutated alongside an additional mutation in the guide sequence: P2+PAM (0.0% indels), P11+PAM (5.7% indels), or P20+PAM (0.0% indels, Figure 2B, Supplementary Table S3). By comparison, we observed slightly increased indel rates when using single nucleotide blocking mutations within the guide sequence in F2 generation dumpy animals (8.1 ± 4.6% indels, $P < 0.05$, Figure 2B, Supplementary Table S3). Furthermore, the position of the substitutions within the guide sequence appears to influence the frequency of indels observed under each blocking condition (Figure 2B, Supplementary Table S3). For example, we observed a low indel rate for the P2 (2.0% indels) and P5 (1.5% indels) substitutions, located near the 3′ end of the guide sequence, whereas we observed increased indel frequency P17 (11.8% indels) and P20 (9.6% indels) substitutions that are closest to the 5′ end of the guide sequence (Figure 2B, Supplementary Table S3). Thus, the expected blocking efficiency of each mutation appears to inversely correlate with the frequency of indel mutations under that blocking condition. In most cases, the indel rate in F2 generation nondumpy animals was increased compared to the respective blocking mutations in their dumpy siblings (Figure 2, Supplementary Table S3) For example, while the P2 mutation led to a 2.0% indel rate in dumpy animals, this rate increased to 18.0% in nondumpy animals (Figure 2, Supplementary Table S3). This suggests that nondumpy animals are biased toward NHEJ-dependent repair pathways compared to their dumpy siblings. This observation suggests that different mechanisms might influence repair of the *dpy-10*-edited haplotypes compared to the haplotypes that are not edited at the *dpy-10* locus.

We were also able to recover HDR-edited animals when a blocking mutation was not incorporated into the repair template. We found that 21.8% of dumpy and 2.3% of nondumpy F2 generation animals carried HDR-edited mutations (Figure 2, Supplementary Table S3), with HDR-editing assessed by the presence of the nonblocking *RsaI* restriction site. Although the HDR-editing rates under the no-blocking condition appeared to be substantially reduced compared to conditions that introduced a blocking mutation (Figure 2, Supplementary Table S3), it was unexpected that any HDR-edited animals could be recovered given that Cas9 was not blocked from targeting the repaired DNA. We defined HDR editing for the no-blocking condition as the incorporation of the *RsaI* restriction site that is located on the 3′ side of the PAM sequence, although it is possible that HDR had occurred without introducing the *RsaI* restriction site. In support of this idea, HDR using ssODN donor molecules has been shown to favor repair in one direction of the PAM depending on which strand the ssODN donor is complementary to Farboud *et al.* (2019). It is therefore possible that our analysis underestimated the frequency of HDR repair when a blocking mutation was not included. These findings suggest that blocking mutations do not appear to be absolutely required to recover HDR-edited animals in *C. elegans*, suggesting that a temporal block might restrict Cas9 from continuing to target the genome after HDR.

We next examined whether there was a correlation between the *tra-2* genotypes of dumpy and nondumpy F2 generation sibling animals that originated from the same F1 hermaphrodite animal (Figure 2D, Supplementary Table S4). Under all blocking conditions that we examined, the majority of F2 generation dumpy animals were HDR-edited, whereas their nondumpy siblings were usually not edited (Figure 2D, Supplementary Table S4). We did not observe any other strong correlations between the two alleles, suggesting that editing of one allele does not affect the probability of editing for the other allele (Figure 2D, Supplementary Table S4). When no blocking mutation was introduced into the repair template, we found that the most frequently observed combination of genotypes was that both dumpy and nondumpy sisters were not edited (Figure 2D, Supplementary Table S4). Thus, editing of each *tra-2* haplotype, one each of maternal and paternal origin, appears to occur independently.

The position of single nucleotide blocking mutations influences the completeness of HDR

Although we observed high HDR-editing rates among all of the blocking conditions that we tested, we found that partial HDR-dependent repair often occurred, where only a subset of the designed mutations was incorporated into the genome (Figure 3A, Supplementary Table S5). For example, in some cases, the blocking mutation was incorporated while the *RsaI* restriction site had not been edited and vice versa (Figure 3A, Supplementary Table S5). We next asked whether the position of blocking mutations influenced the efficacy of HDR (Figure 3A, Supplementary Table S5). For the purpose of this analysis, we only considered genotypes where partial or complete HDR-editing had occurred (Figure 3A, Supplementary Table S5). We quantified the percentage of HDR-edited genotypes that contained a designed blocking mutation, the *RsaI* restriction site, or both blocking and *RsaI* mutations (Figure 3A, Supplementary Table S5). We found that blocking conditions where the PAM was mutated led to increased incorporation of both the blocking mutation and *RsaI* restriction site among the HDR-edited animals (Figure 3A, Supplementary Table S5). When only the PAM was mutated, the majority of HDR-edited chromosomes contained both the PAM blocking mutation and the *RsaI* restriction site (97.8% both mutations), while a small percentage contained only the *RsaI* restriction site (2.2% *RsaI* only) (Figure 3A, Supplementary Table S5). Interestingly, all HDR-edited chromosomes that we examined for the P2+PAM blocking condition were edited for both the blocking mutation and the *RsaI* restriction site (100% both mutations), while the P2 blocking condition itself resulted in less frequent incorporation of both blocking mutations and the *RsaI* restriction site (36.2% both mutations) and commonly resulted in partial repair of only the blocking mutation (31.9% P2 only) or the *RsaI* restriction site (31.9% *RsaI* only) (Figure 3A, Supplementary Table S5). We observed a similar trend for the P11+PAM or P20+PAM blocking conditions compared to

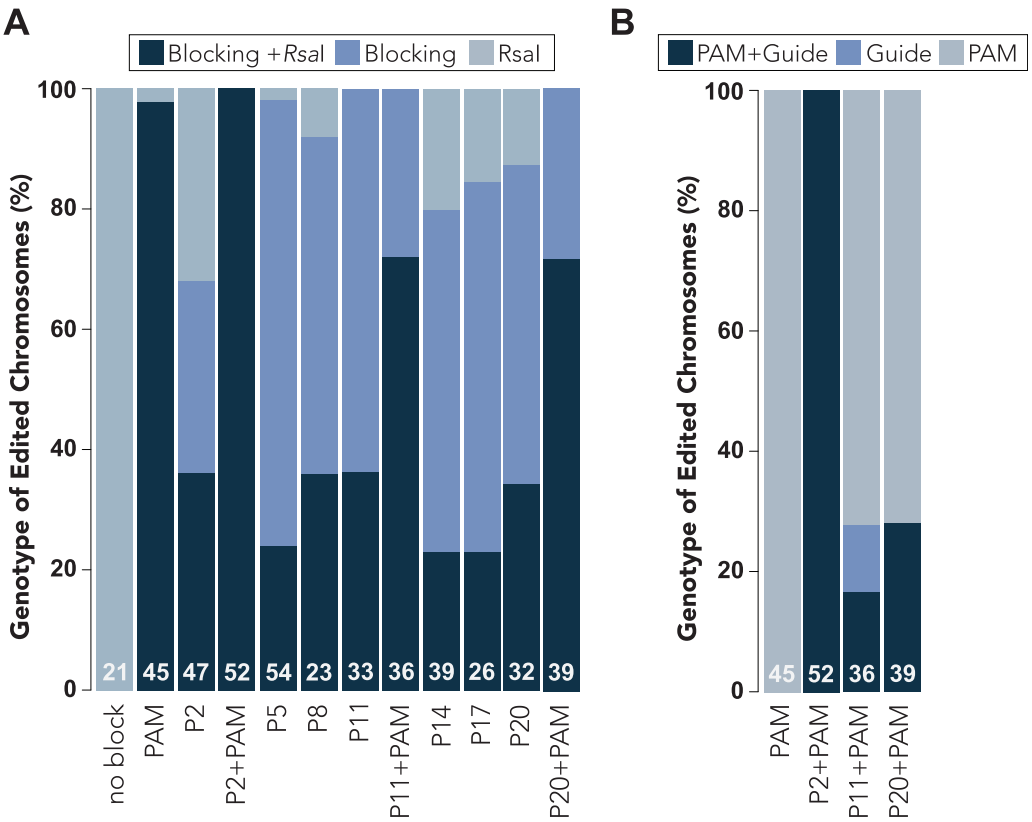

Figure 3 Differences in HDR Editing Efficiency Under Different Blocking Conditions. (A) Percent HDR-edited chromosomes containing mutations for the nonblocking *RsaI* restriction enzyme cutting site, blocking mutation, or both blocking and *RsaI* mutations. For genome edits that introduce more than one blocking mutation into the PAM and guide sequence, we scored the presence of at least one blocking mutation (*i.e.*, PAM, guide, or both). (B) Percent HDR edited chromosomes containing blocking mutations in the PAM sequence, guide sequence, or both PAM and guide sequences. (A,B) All results were determined through Sanger sequencing of singled F2 generation animals. Data are subset from the data presented in Figure 2, B and C and includes the "edited" chromosomes from F2 generation Dumpy and nondumpy animals. White text at the bottom of each stacked bar indicates the number (*n*) of animals that were sequenced.

the P11 or P20 blocking conditions respectively, where complete HDR of both blocking mutations and the *RsaI* restriction site was more frequent when the PAM was also mutated (Figure 3A, Supplementary Table S5). While we cannot be certain why the presence of PAM blocking mutations led to increased frequency of complete HDR repair compared to blocking mutations in the guide sequence, we hypothesize that partial HDR repair could reflect incomplete blocking of Cas9. This, in turn, could lead to Cas9 recutting of repaired DNA and increased frequency of inaccurate HDR as repair is attempted multiple times. We also observed that HDR appeared to occur in an asymmetric fashion, favoring blocking mutations over *RsaI* site incorporation. For example, when P20 was used as a blocking mutation we observed more frequent incorporation of the P20 mutation (87.5% P20 edited) than the *RsaI* restriction site (46.9% *RsaI* edited), despite *RsaI* being located closer to the expected Cas9-generated break site (Figure 3A, Supplementary Table S5). This observation suggests that edits that do not block Cas9 from recutting (such as introduction of the *RsaI* site) may result in multiple cleavage and repairs, thus ultimately favoring repair events that incorporate the blocking mutations. However, the presence of *RsaI* edits that do not include blocking mutations further supports the existence of a temporal block that prevents Cas9 from recutting the repaired template.

Since previous reports have shown that the efficiency of HDR editing is inversely correlated with distance to the Cas9-generated break site (Arribere *et al.* 2014; Inui *et al.* 2014; Paix *et al.* 2014, 2015; Ward 2015), we asked whether the distance of blocking mutations from the break site might be confounded with their actual ability to block Cas9. In other words, the P2 blocking mutation might increase the frequency for recovery of HDR-edited animals compared to the P20 blocking mutation because it is closer to the dsDNA break site and is therefore more likely to incorporate during repair, rather than the P2 mutation blocking Cas9 more effectively than P20. To address this, we examined how frequently partial or complete HDR occurred when using repair templates that mutated one nucleotide within the guide sequence as well as the PAM domain to ensure that Cas9 was equally blocked under each condition (P2+PAM, P11+PAM, and P20+PAM) (Figure 3B, Supplementary Table S6). When both the PAM and P2 mutations were introduced, we found that all of the edited chromosomes that we examined contained both PAM and P2 mutations (100% both edited) (Figure 3B, Supplementary Table S6). However, when the PAM was mutated alongside the P11 or P20 mutations, we found that partial HDR repair had often occurred. In particular, we found that the majority of HDR-edited chromosomes contained only the PAM blocking mutation when either P11+PAM (72.2% PAM only) or the P20+PAM (71.8% PAM only) repair templates had been used (Figure 3B, Supplementary Table S6). Only a small fraction of HDR-edited chromosomes contained both the guide blocking mutation and the PAM mutation for the P11+PAM (16.6% both edited) or P20+PAM (28.2% both edited) mutations (Figure 3B, Supplementary Table S6). Therefore, the distance of blocking mutations from the dsDNA break site, which

is located near the 3′ end of the guide sequence, appears to influence the rate at which they are incorporated via HDR. Blocking mutations located farther away from the dsDNA break site may not always be incorporated through HDR, leading to an overall decrease in HDR-editing efficiency since Cas9 can re-target the partially repaired chromosome. Despite the reduced incorporation of the more distant blocking mutations, the overall high efficiency of obtaining desired edits (Figure 2) strongly supports practical use of single nucleotide blocking mutations when PAM mutations are not possible.

Single nucleotide guide substitutions effectively, although not completely, block Cas9

Having determined that single nucleotide blocking mutations allow for recovery of HDR-edited animals (Figure 2), we next asked how effective each of blocking mutations might be in preventing Cas9 from targeting the *tra-2* genomic locus after HDR occurred. To address this question, we took advantage of the *tra-2* HDR-edited animals that we generated (Figure 2), containing blocking mutations as well as the *Rsa*I restriction enzyme cutting site. We reasoned that if the blocking mutations built into the *tra-2* locus prevent Cas9 from targeting the mutated sequences, then re-injection of Cas9 and the same guide RNA, perfectly matched to the wild-type *tra-2* genomic sequence, should not lead to editing of the mutated *tra-2* loci (Figure 5A). To examine whether re-editing of *tra-2* could occur under any of the blocking conditions, we designed a repair template that would revert *tra-2* back to the wild-type genomic sequence (Figure 4A). Because the HDR-edited strains contain blocking mutations and the *Rsa*I restriction enzyme site, reversion of *tra-2* back to the wild-type sequence will result in removal of the *Rsa*I restriction enzyme site (Figure 4A). Furthermore, as the *Rsa*I restriction enzyme site is located immediately downstream of the *tra-2* PAM (Figure 2A), indel mutations might also be expected to disrupt the *Rsa*I site. On the other hand, if Cas9 is completely blocked from generating a dsDNA break at the mutated *tra-2* locus, then all of the F1 progeny post-injection should still contain the *Rsa*I restriction enzyme site. Importantly, any animal now lacking the *Rsa*I site must have been targeted by Cas9 for genome editing to have occurred, which would indicate that Cas9 was not completely blocked under that condition. To test whether the position of blocking mutations within the guide sequence influenced their blocking efficacy, we examined the *Rsa*I reversion efficiencies of the P2, P11, and P20 mutations (Figure 4A). As a positive control, we reverted the *Rsa*I site in a strain that did not contain any Cas9 blocking mutations ("no-block"), which would still be expected to be targeted by Cas9 loaded with the wild-type guide (Figure 4A). Because the PAM is absolutely required for Cas9 activity (Mojica *et al.* 2009; Marraffini and Sontheimer 2010; Jinek *et al.* 2012; Sashital *et al.* 2012), we attempted to revert the *Rsa*I site in PAM-edited animals as a negative control (Figure 4A).

We used *dpy-10* coconversion to enrich for genome-edited animals and examined whether F1 generation roller and dumpy animals contained the *tra-2 Rsa*I restriction site (Figure 4B, Supplementary Table S7). We calculated the haplotype *Rsa*I reversion rate by dividing the number of reverted haplotypes (one for heterozygous reverted animals and two for homozygous reverted animals) by the total number of haplotypes that were examined. As expected, we observed robust reversion of the *Rsa*I restriction site in the no-blocking control and never observed reversion of the *Rsa*I site in PAM-edited animals (Figure 4B). For the no-blocking control, we found that the *Rsa*I reversion rates of F1 generation dumpy (32% haplotypes reverted) and roller (25%

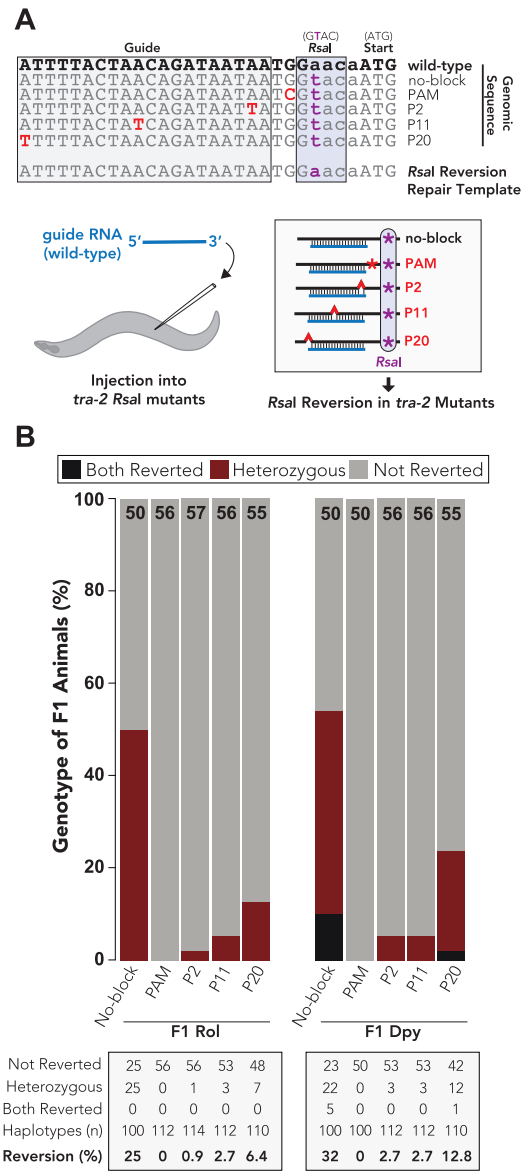

	No-block	PAM	P2	P11	P20	No-block	PAM	P2	P11	P20
Not Reverted	25	56	56	53	48	23	50	53	53	42
Heterozygous	25	0	1	3	7	22	0	3	3	12
Both Reverted	0	0	0	0	0	5	0	0	0	1
Haplotypes (n)	100	112	114	112	110	100	100	112	112	110
Reversion (%)	**25**	**0**	**0.9**	**2.7**	**6.4**	**32**	**0**	**2.7**	**2.7**	**12.8**

Figure 4 Single nucleotide guide substitutions effectively block Cas9 in a position-dependent manner. (A) Top: sequence alignment of *tra-2* genome-edited animals that were re-injected to revert the *tra-2 Rsa*I restriction site back to the wild-type genomic sequence. Note that the same *Rsa*I reversion repair template was injected into all strains and is also expected to revert the blocking mutations back to the wild-type genomic sequence. As the *Rsa*I cutting site is located nearby the expected cutting site for Cas9, both *Rsa*I reversions and relatively small deletions would be expected to eliminate *Rsa*I cutting for edited alleles. Because some mutations would not disrupt *Rsa*I digestion, this analysis underestimates the true mutation rate. Bottom: schematic representation of the experimental procedure. Animals containing tra-2 RsaI mutations are injected with a wild-type guide. As the tra-2 mutants are genome-edited, the wild-type guide sequence is not perfectly paired to the mutant genomic sequences (B) Quantification of F1 generation roller and dumpy animals digested with *Rsa*I. "Both reverted" indicates that the singled F1 animals were homozygous for *Rsa*I reversion back to wild type (did not digest with *Rsa*I). "Heterozygous" animals showed both patterns of *Rsa*I digestion. "Not reverted" indicates that the animals underwent full *Rsa*I digestion and were not reverted back to wild type. Black text at the top of each stacked bar indicates the number (*n*) of F1 animals that were digested with *Rsa*I. Table (bottom) shows number of F1 generation animals corresponding to each genotype. Reversion (%) illustrates the haplotype editing frequency, which was calculated by dividing the total number of edited haplotypes (two in "both reverted" and one in heterozygous animals) from the total number of haplotypes examined.

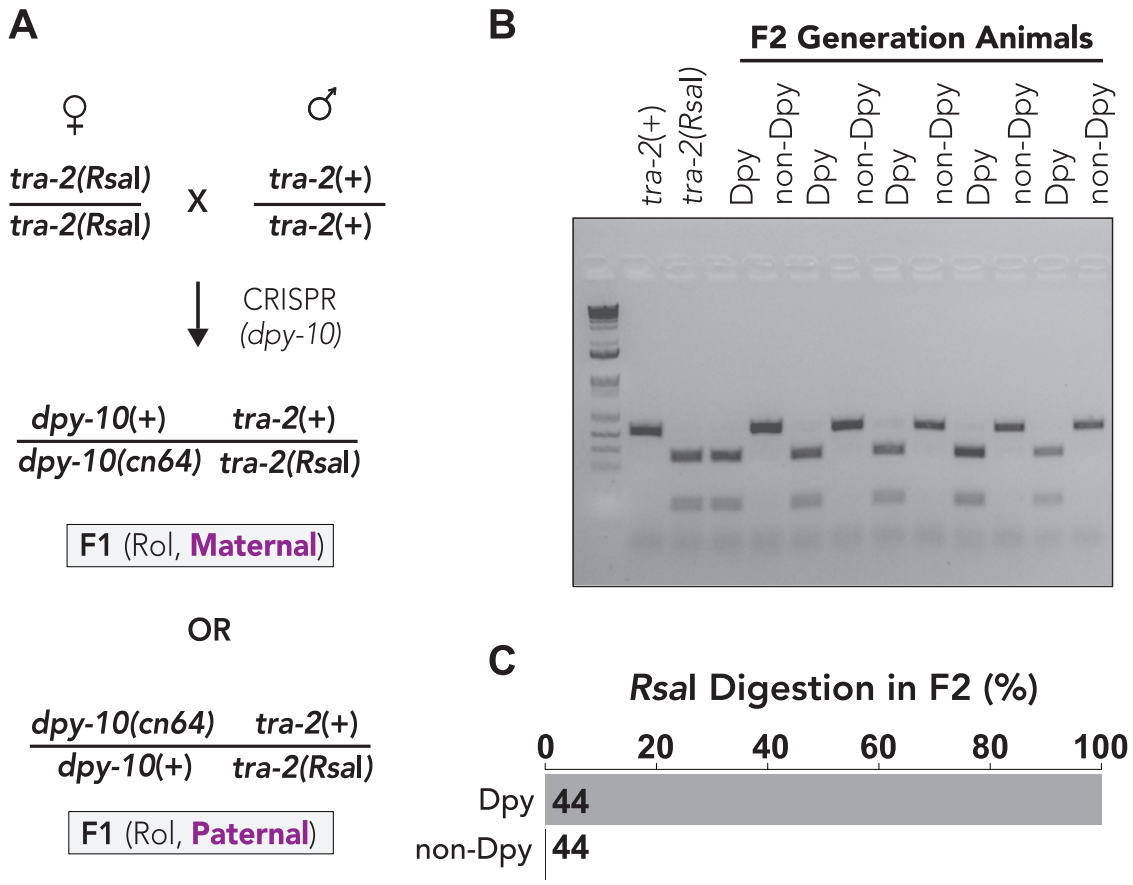

Figure 5 Analysis of maternal and paternal genome editing rates. (A) Mating strategy to test frequency of maternal *vs* paternal genome editing. Hermaphrodite animals containing the *tra-2 RsaI* (no-blocking) restriction enzyme site were crossed to wild-type males and allowed 24 h to mate. Mated hermaphrodites were subsequently injected to generate the *dpy-10(cn64)* variation. F1 generation rollers contain a single edit for the *dpy-10(cn64)* allele and a maternally provided allele of *tra-2* that contains the *RsaI* site. For maternal edits, the F2 generation dumpy animals will be homozygous for the *tra-2* allele containing the *RsaI* restriction site. In the case of paternal edits, the nondumpy animals will be digested with *RsaI*. (B) Representative agarose gel illustrates differences in editing efficiencies of maternal and paternal genomes. Wild-type animals are not digested with *RsaI* and migrate as a single band whereas animals containing the *tra-2(RsaI)* allele are digested and migrate as two bands. (C) Quantification of *RsaI* digestion rates in F2 generation dumpy and nondumpy animals. *RsaI* digestion in dumpy animals is indicative of maternal genome editing of *dpy-10*. Black number indicates the number (*n*) of animals that were digested with *RsaI*. One dumpy and one nondumpy animal was screened per F1 generation animal.

haplotypes reverted) animals were similar, although we only observed homozygous-reverted animals in F1 generation dumpy animals (Figure 4B, Supplementary Table S7). The increased prevalence of homozygous-reverted animals in F1 generation dumpy animals might not be surprising, since the dumpy phenotype indicates that homozygous editing of the *dpy-10* genomic locus had also occurred. We found that the P2 blocking condition was highly effective at blocking Cas9, as only a small percentage of F1 generation dumpy (2.7% haplotypes reverted) or roller (0.9% haplotypes reverted) animals had reverted the *RsaI* site (Figure 4B, Supplementary Table S7). Similarly, the P11 mutation was highly effective at blocking Cas9 and resulted in only a low frequency of *RsaI* reversion in F1 generation dumpy (2.7% haplotypes reverted) and roller (2.7% haplotypes reverted) animals (Figure 4B, Supplementary Table S7). Despite increased *RsaI* reversion frequency in P20 blocking mutants for both F1 generation dumpy (12.8% haplotypes reverted) and roller (6.4% haplotypes reverted) animals (Figure 4B, Supplementary Table S7), the P20 blocking mutation blocked Cas9, as the *RsaI* reversion rates were much lower in P20 mutants compared to no-block controls (Figure 4B, Supplementary Table S7). Therefore, consistent with previous reports (Jinek *et al.* 2012; Cong *et al.* 2013; Fu *et al.* 2013; Hsu *et al.* 2013; Mali *et al.* 2013; Pattanayak *et al.* 2013; Zhang *et al.* 2015), the position of single nucleotide guide substitutions appears to influence their blocking efficacy where substitutions located proximal to the 3′ end of the guide are more effective at blocking Cas9 (Figure 4B, Supplementary Table S7). Interestingly, although we observed similar HDR editing rates for the P11 (75.7% HDR-edited in Dumpy animals, Figure 2, Supplementary Table S3) and P20 mutations (66.6% HDR-edited in Dumpy animals, Figure 2, Supplementary Table S3), P11 was more effective at blocking Cas9 than P20 (Figure 4B, Supplementary Table S7). This discrepancy between blocking efficacy and HDR editing rates further supports the idea that perhaps a temporal effect contributes toward allowing for robust genome editing when Cas9 is not completely blocked. Collectively, these findings show that single nucleotide substitutions in the guide sequence effectively, albeit not completely, block Cas9 after HDR occurs, and that conditions where Cas9 is not completely blocked still allow for efficient genome editing in *C. elegans*.

Editing of maternal haplotypes occurs at greater frequency than editing of paternal haplotypes

Given that we observed significantly higher HDR-editing rates of the *tra-2* locus in *dpy-10*-edited haplotypes compared to non-*dpy-10* haplotypes (Figure 2, B–D), we asked whether there could be

differences in the HDR-editing efficiencies of each parentally contributed haplotype. To determine the HDR editing rates of each parental haplotype, we used a mating-based approach to differentiate between maternal and paternal haplotypes (Figure 5A). We crossed wild-type males to *tra-2* mutant hermaphrodites that carried the *RsaI* restriction site just upstream of the *tra-2* coding sequence (Figure 4A). We then injected the mated animals with Cas9 RNP complex to generate the *dpy-10(cn64)* variation (Figure 5A). Because *dpy-10* and *tra-2* are genetically linked and not expected to independently assort, the resulting F1 generation roller animals will have two possible haplotype arrangements for the *dpy-10* and *tra-2* mutations (Figure 5A). One possible F1 genotype will have the maternally contributed *tra-2* mutation (*RsaI* site) on the same chromosome as the newly introduced *dpy-10(cn64)* mutation and another possible F1 genotype would have the *tra-2* and *dpy-10* mutations on different chromosomes (Figure 5A). Both of these possible haplotype arrangements can be differentiated in the F2 generation by examining whether the dumpy or nondumpy progeny contain the *tra-2 RsaI* restriction site (Figure 5A). If maternal editing of *dpy-10* occurs, then the F2 generation dumpy animals would be homozygous for the *tra-2 RsaI* allele whereas the nondumpy F2 generation animals would be homozygous for the paternally provided wild-type *tra-2* allele (Figure 5A). If editing occurred in the paternal genome, then the F2 generation dumpy animals would be homozygous for the wild-type *tra-2* allele that lacks the *RsaI* cut site (Figure 5A). We genotyped one F2 generation dumpy and one F2 generation nondumpy animal per F1 generation roller animal ($n = 44$ animals). In all F2 generation animals that we examined, *RsaI* digestion occurred only in dumpy animals, supporting the idea that editing of the maternal genome is strongly preferred over paternal genome editing (Figure 5, B and C). Thus, we conclude that the distinct *tra-2* HDR rates we previously observed in dumpy *vs* nondumpy F2 generation animals (Figure 2, B and C) are likely due to differences in the editing efficiencies of each paternal genome, where dumpy animals are likely homozygous for the maternally provided haplotype and nondumpy animals are likely homozygous for the paternally provided haplotype.

Selection of maternally provided haplotypes using balancer chromosomes to mutate the *let-7* miRNA in a scarless fashion

As we observed increased HDR editing efficiency of maternally provided genomes compared to paternally provided genomes (Figure 5), we devised a strategy to select for the maternally provided haplotypes postinjection (Figure 6A). Our approach was to label paternally provided chromosomes prior to injection by mating wild-type hermaphrodite animals to males expressing fluorescently labeled balancer chromosomes (Figure 6A). Importantly, the use of balancer chromosomes restricts recombination between the maternally provided wild-type chromosome and the paternally provided balancer chromosome. This allows for segregation of each parental haplotype in subsequent generations and easily homozygoses for the desired edit, thereby reducing screening efforts postinjection (Figure 6A). We used this strategy, along with single nucleotide blocking mutations to mutate the *let-7* miRNA in a scarless fashion. As loss of *let-7* function is lethal (Reinhart *et al.* 2000), this strategy also allowed us to immediately maintain deleterious *let-7* mutations in a balanced, heterozygous genetic background, using the *tmc24* balancer chromosome (Dejima *et al.* 2018). Because the *tmc24* balancer contains a *pmyo-2::Venus* fluorescent marker that is pharyngeal expressed (Dejima *et al.* 2018), F1 generation cross-progeny should be fluorescently labeled whereas self-progeny would not be labeled (Figure 6A). In the subsequent F2 generation, animals without expression of pharyngeal Venus should be homozygous for the maternally provided *let-7* haplotype as the non-Venus animals lack the paternally provided *tmc24* chromosome (Figure 6A).

We targeted *let-7* using a guide sequence overlapping with the mature *let-7* miRNA sequence and used ssODN repair templates to introduce single nucleotide blocking mutations into the endogenous *let-7* locus. As a proof of principle, to demonstrate our ability to create scarless edits within nonprotein-coding portions of the genome using a single nucleotide mismatch within the guide region, we aimed to generate a P6 blocking mutation, which recapitulates the classical *let-7(n2853)* hypomorphic mutation. *let-7(n2853)* disrupts the *let-7* seed sequence and leads to dysregulation of *let-7* mRNA targets in a temperature sensitive manner (Reinhart *et al.* 2000; Vella *et al.* 2004) (Figure 6B). We also designed two nonseed mutations as controls: one located within the PAM domain that is expected to completely block Cas9 and a second nonblocking mutation located downstream of the PAM (Figure 6B). We used *dpy-10* coconversion to enrich for genome-edited animals and singled both F1 generation roller and dumpy animals (Figure 6A). We then sequenced non-Venus F2 generation animals to examine how each blocking condition affected HDR efficiency (Figure 6A).

We observed high HDR-editing rates (60.7% HDR-edited) and low indel rates (10.7% indels) when the PAM was mutated (Figure 6C). We observed comparable rates of HDR-editing (56.7% HDR-edited) when P6, which recapitulates the *let-7(n2853)* mutation (Figure 6B), was used as the blocking mutation (Figure 6C). Although the HDR-editing rates were similar for the PAM and P6 blocking conditions, the indel rate was twice as high for the P6 blocking mutation (23.3% indels) compared to the PAM mutation (10.7% indels) (Figure 6C). The increased indel rate observed under P6 blocking conditions might indicate that P6 does not completely block Cas9. Consistent with this idea, we found that the no-blocking condition led to high frequency of indel mutations (40.7% indels) and low rate of HDR-editing (3.7% HDR-edited) (Figure 6C).

Interestingly, we did not observe a similar increase in indel rates for the *tra-2* no-blocking condition (Figure 2, B and C), suggesting that there may be gene-specific or guide-specific differences in indel rates *vs* HDR-editing rates. Importantly, we were able to isolate a small percentage of *let-7* HDR-edited animals, even when the ssODN repair template did not contain a blocking mutation (Figure 6C). This observation supports the idea that in situations where no blocking mutations can be designed, desired edits can nonetheless be obtained, albeit at a low frequency.

Many microRNAs, including *let-7*, are members of microRNA families that share the same seed sequence and are therefore expected to target similar mRNA sequences (Lewis *et al.* 2003; Lim *et al.* 2003). As a result of sharing the same seed sequence, many members of microRNA families often exhibit functional redundancy with other family members (Abbott *et al.* 2005; Miska *et al.* 2007; Alvarez-Saavedra and Horvitz 2010). As a further proof of principle, to demonstrate the utility of selecting for maternal chromosomes via paternally provided balancers, we aimed to recapitulate the *let-7(n2853)* variation in a genetic background devoid of the other three major *let-7* family members: miR-48, miR-84, and miR-241. Such strain has been difficult to generate using conventional genetic methods, since the *let-7* and miR-84 microRNAs are genetically linked and complete loss of *let-7* activity is lethal (Reinhart *et al.* 2000). To generate a strain containing mutations in all four *let-7* family members, we crossed *tmc24*

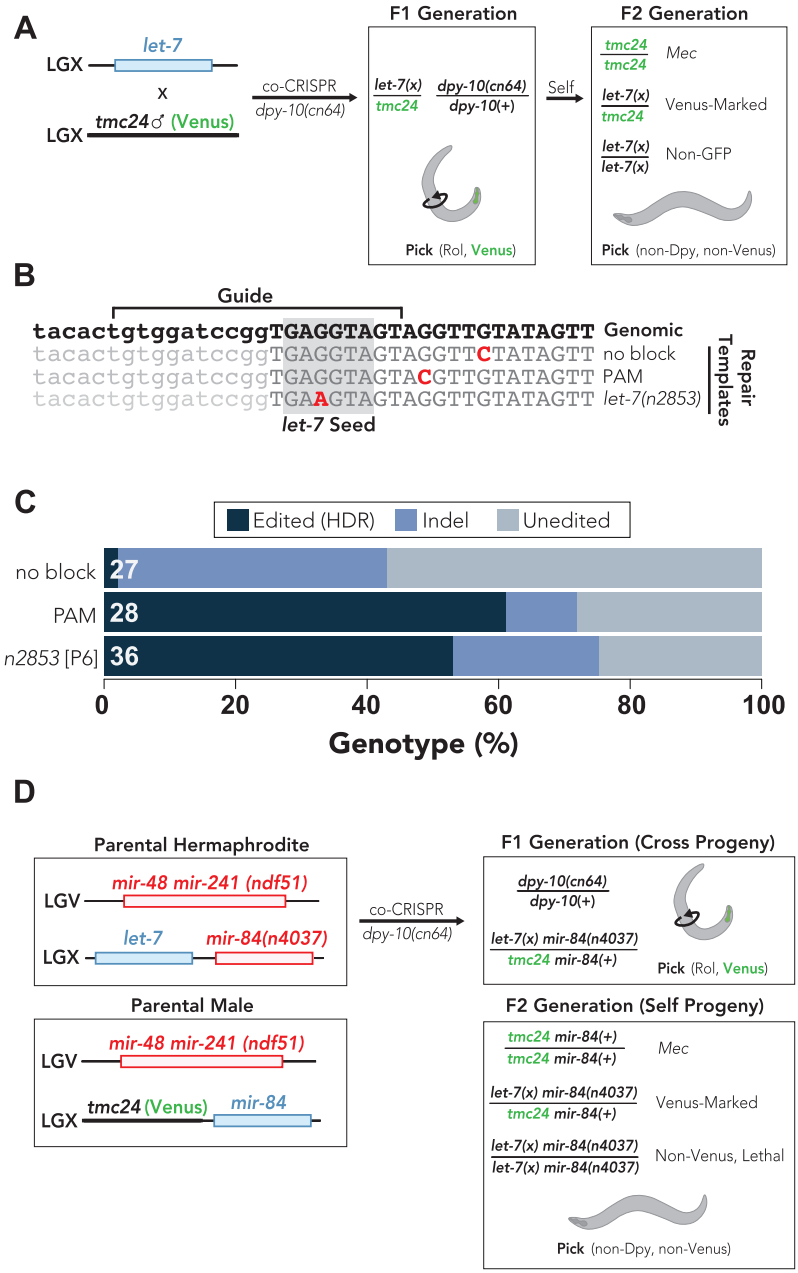

Figure 6 Selection of maternally provided haplotypes using balancer chromosomes. (A) Mating wild-type hermaphrodites to males carrying balancer chromosomes before injection allows for differentiation of maternal and paternal haplotypes for genes that are within the balanced interval and takes advantage of the more frequent maternal edits. The *tmc24* balancer covers an interval on the right side of LGX that includes the *let-7* miRNA and contains a Venus-marked transgene expressed in the pharynx. Prior to injection, *tmc24* males were mated to wild-type hermaphrodites and then subjected to co-CRISPR to mutate the *let-7* and *dpy-10* genes. F1 generation cross progeny will contain pharyngeal Venus, and roller animals were successfully mutated in the *dpy-10* gene. Because *dpy-10* and *let-7* are not on the same chromosome, nondumpy animals can be isolated in the F2 generation to remove the *dpy-10(cn64)* allele. Homozygous animals for the *tmc24* balancer have a mechanosensory variant (Mec) phenotype, which can differentiate homozygous and heterozygous animals. Non-Venus F2 generation animals do not contain the paternally contributed *tmc24* balancer and are therefore homozygous for the maternally contributed *let-7* allele. (B) Alignment of *let-7* genome edits generated in this study. The wild-type genomic sequence is shown on the top line. The mature *let-7* miRNA is indicated by uppercase lettering and the *let-7* seed sequence is boxed in gray. Changes to the genomic sequence are indicated in red text. Introduction of the *let-7* seed mutation equivalent to the *let-7(n2853)* allele, which leads to a single nucleotide variation 6 bases away from the 3′ end of the guide sequence ("P6"). (C) Percent *let-7* genotypes observed for F2 generation non-Venus animals that were singled from F1 generation Venus-positive rollers. Indels were defined as any insertion or deletion mutation, regardless of whether editing through HDR may have occurred. Unedited animals had no apparent changes compared to the wild-type *let-7* sequence. All results were determined through Sanger sequencing. White text at the left of each stacked bar indicates the number (n) of animals that were sequenced. (D) Strategy to generate *let-7* family *mir-48 mir-241(nDf51); mir-84(n4037) let-7(n2853)*-equivalent quadruple mutant. Hermaphrodite animals containing *mir-48 mir-241* and *mir-84* deletions are crossed to *ndf51; tmc24* males prior to injection, which homozygoses *ndf51* in subsequent generations. Note that mir-84 is on chromosome X and is genetically linked to the tmc24 balancer. While *mir-84* is not on the balanced interval covered by *tmc24*, *mir-84* and *tmc24* are not expected to independently assort during meiosis, which effectively maintains the *mir-84* deletion as heterozygous. We identified *let-7(n2853)-equivalent* mutants by singling F1 generation rollers and sequencing the non-Venus F2 generation progeny. The non-Venus quadruple mutants were invariably lethal at all temperatures that we tested but can be maintained by picking heterozygous animals expressing pharyngeal Venus.

balancer males to hermaphrodite animals containing deletions of *mir-48*, *mir-84*, and *mir-241* (Figure 6D). We then performed co-CRISPR of *let-7* and *dpy-10* to recapitulate the *let-7(n2853)* mutation (Figure 6D). As *let-7* and *mir-84* are both located on the X chromosome, F1 generation cross-progeny will have a paternally provided *tmc24* chromosome and a maternally provided chromosome that contains a mir-84 deletion, which we targeted for the *let-7* editing (Figure 6D). We then sequenced F2 generation non-Venus animals and identified animals containing maternal *let-7(n2853)* mutations. Using this strategy, we were able to create a stable strain that contains homozygous deletions in *mir-48* and *mir-241 (nDf51)* and the *mir-84(n4037)* deletion and *let-7(n2853*-equivalent) mutation balanced by *tmc24* in a heterozygous state.

Collectively, these findings demonstrate that single nucleotide substitutions within the guide RNA targeting sequence can be used to effectively mutate miRNAs through HDR in an otherwise scarless fashion. Furthermore, we propose that balancer chromosomes can be used to select for maternally provided haplotypes and introduce deleterious mutations directly into a balanced heterozygous background in a single injection step.

The use of *dpy-10(cn64)* coinjection may further facilitate the single-step injection approach, since F1 generation rollers containing a single *dpy-10(cn64)* edited chromosome are more likely to only contain a single edit at a second locus. Previous strategies used in *C. elegans* to introduce potentially lethal genome edits directly into balanced genetic backgrounds have relied on two-step editing approaches, where the first edit introduces a nascent PAM to a gene of interest that can be specifically edited in a second injection after being crossed to a balancer chromosome that lacks the nascent PAM (Dejima *et al.* 2018; Duan *et al.* 2020). As nearly 90% of the *C. elegans* genome is covered by balancer mutations (Dejima *et al.* 2018), our strategy can be used to target most *C. elegans* genes in a single step editing approach, eliminating the need for extensive postinjection screening.

Discussion

Strategies for designing Cas9 blocking mutations in *Caenorhabditis elegans*

In this study, we performed a detailed analysis of a single guide-target pair to determine the blocking efficacy of single nucleotide substitutions within the guide region of the donor molecule. As we only tested a single guide-target pair, it is possible that some of our conclusions do not apply to all guide-target interactions. However, our findings that single nucleotide substitutions are sufficient to allow recovery of HDR-edited animals, and that blocking mutations are not strictly required for recovery of HDR-edited animals are also supported by our analysis of the *let-7* locus. Furthermore, we have routinely used single nucleotide substitutions in the guide-binding region to generate additional genome-edited strains, supporting that this approach is broadly effective across several genetic loci (Supplementary Figure S1). Mutating the PAM domain remains the most effective way to block Cas9 and leads to the highest HDR editing rates (Figure 7A). However, when the desired mutation overlaps with the guide sequence, additional blocking mutations are not necessary to recover HDR edited animals, which can facilitate scarless HDR editing (Figure 7B). For protein-coding genes, it is also possible to introduce silent blocking mutations into the guide sequence, ideally close to the 3′ end of the guide, when silently mutating the PAM is not possible (Figure 7C). For edits that do not overlap with the guide sequence or PAM, it is possible to forego the use of blocking mutations in order to recover animals in an otherwise scarless genetic background (Figure 7D). The ability to recover HDR edited animals without including a blocking mutation suggests that a temporal block to Cas9 activity exists in *C. elegans*, preventing Cas9 recutting of the repaired genomic region (Figure 7E). Cas9 activity might be highest in the distal end of the maternal germline, since this is where Cas9 RNP complexes are injected (Figure 7E). The temporal block to Cas9 activity might result from degradation of the injected Cas9 RNP complexes or dilution of Cas9 activity as germ cells passage through the maternal germline from distal end to proximal end (Figure 7E). Collectively our findings expand the repertoire of possible genome edits in *C. elegans* and should facilitate analysis of noncoding regulatory sequences without the need for extraneous Cas9 blocking mutations.

Differences in maternal *vs* paternal genome editing rates in *C. elegans*

We found that the HDR editing rates of *tra-2* were much higher for the haplotypes that contained the *dpy-10(cn64)* allele compared to the haplotypes that were not edited for *dpy-10* (Figure 2). Given that the Cas9 RNPs are injected into the maternal germline of hermaphrodite animals, it seemed likely that editing of the maternally provided haplotype is preferred over editing of the paternally provided haplotype. Indeed, several others have speculated that editing of maternal haplotypes is preferred in *C. elegans* (Arribere *et al.* 2014; Kim *et al.* 2014; Paix *et al.* 2014, 2016), although both paternal and maternal germ cells are competent for HDR (Clejan *et al.* 2006). We used a mating-based approach that allowed us to quantify the editing rates of maternal and paternal haplotypes and demonstrated that maternal editing was preferred over paternal editing (Figure 5). This is in contrast to a recent study, which suggested that paternal genome (embryonic) editing is preferred over maternal editing (Farboud *et al.* 2019). A key difference in our experimental design was that we were able to assess maternal *vs* paternal genome editing in a single injection step, whereas previous studies have assessed maternal and paternal editing in separate injections (Farboud *et al.* 2019). Farboud and colleagues performed two injections, where each injection was designed to specifically target one parental haplotype. However, the allele-specific editing was predicated on the assumption that a single nucleotide mismatch in the guide-binding region (equivalent to "P2") was sufficient to completely block Cas9, which our findings suggest is not accurate. Furthermore, Farboud *et al.* used a much higher concentration of Cas9 (15 μM) than we used in this study (2.65 μM), which could have allowed Cas9 to persist longer in the *C. elegans* germline and lead to more effective editing of paternally provided haplotypes. Nevertheless, it is also possible that there could be gene-specific differences in haploid genome editing efficiency.

Taking advantage of the preference for maternal editing, we were able to select for the maternally provided chromosomes using balancer chromosomes that restrict recombination between the maternal and paternal chromosomes. By mating hermaphrodite animals to males containing a balancer chromosome before injection, the maternally provided nonbalancer chromosome of coedited F1 roller animals is more likely to be edited. Because typical balancer chromosomes contain a fluorescent or physical marker to identify animals harboring the balancer, nonmarked animals can be easily identified and should be homozygous for the maternally provided haplotype. Homozygosing for the edited, maternally provided chromosome would homozygose for the mutation of interest and therefore reduce molecular method-based screening. It would also be possible to recover edited

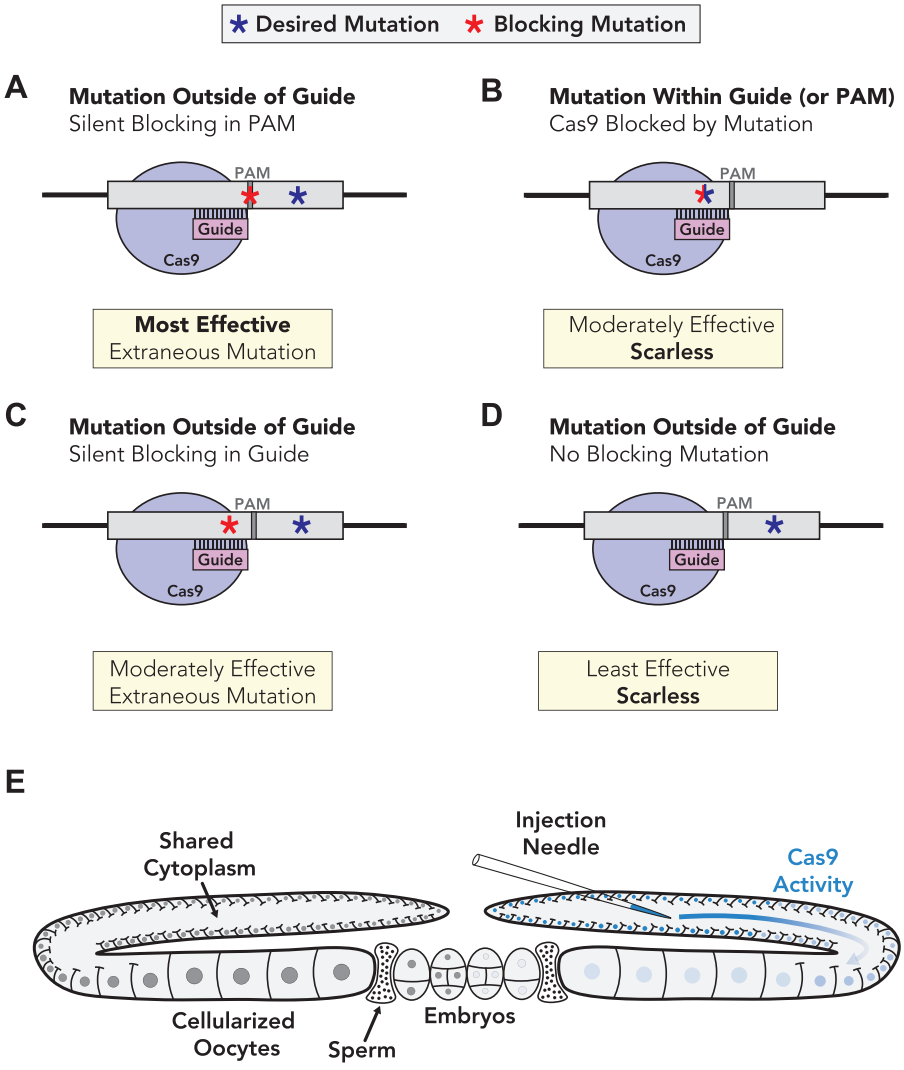

Figure 7 Strategies for creating Cas9 blocking mutations in *C. elegans*. (A–D) Examples of strategies for introducing mutations to block Cas9 in *C. elegans*. (A) The most straightforward method to blocking Cas9 is to introduce a silent mutation into the PAM domain. In an ideal scenario, the desired mutation disrupts the PAM domain and consequently blocks Cas9, which would lead to a "scarless" edit. Whenever possible, mutating the PAM completely blocks Cas9 and leads to the highest relative HDR rates. (B) When the intended mutation overlaps with the guide targeting sequence, additional blocking mutations are not required, although are slightly less effective than PAM mutations. An advantage of this method is that the desired mutation also serves as the blocking mutation, leading to a scarless edit. (C) For protein-coding genes where the PAM cannot be silently mutated, a silent single base substitution in the guide targeting sequence is sufficient to allow for recovery of HDR-edited animals. (D) When silent mutations cannot be engineered into the guide or the desired mutation does not overlap with the guide/PAM sequences, it is possible to recover HDR-edited animals without including a blocking mutation in *C. elegans*. While this approach has the advantage of being scarless, it is the least effective in terms of HDR-editing rates. (E) Model for temporal block to genome editing in *C. elegans*. Cas9 RNPs and single-stranded DNA repair templates are injected into the distal end of the maternal germline (right gonad arm). Cas9 activity is attenuated as it passes from the injection site toward the proximal gonad. This might be due to two different possibilities: (1) Cas9 RNPs are unstable and/or degraded over time or (2) Cas9 is able to target chromosomes located in the distal germline more effectively than chromosomes in the proximal germline. In either case, Cas9 activity appears to be temporally restricted, allowing for HDR repair even when blocking conditions do not completely block Cas9.

animals by injecting directly into balanced, heterozygous animals without mating prior to injection. F1 generation animals could be screened for heterozygosity and would carry a mutation on either the balancer chromosome or the nonbalanced chromosome. If the edit was not on the balancer chromosome, F2 generation animals lacking the balancer chromosome would be homozygous for the desired edit. As most of the *C. elegans* genome is covered by balancer chromosomes (Dejima *et al.* 2018), this approach can be broadly applied to most *C. elegans* genes and has the added advantage of introducing potentially deleterious mutations directly into a balanced genetic background.

Single nucleotide substitutions are sufficient to allow recovery of HDR-edited animals in *C. elegans*

In this study, we demonstrate that a single nucleotide mismatch at any point in the guide sequence can block Cas9 and can be reliably used to recover HDR-edited animals. However, despite the fact that these single nucleotide blocking mutations are sufficient to allow for recovery of HDR-edited animals, we show that Cas9 was still able to target genomic sequences containing a single mismatch to its guide RNA, including the P2 substitution (Figure 4). These data provide direct evidence that off-target

cutting can occur in *C. elegans*, in contrast to previous speculation that off-target cutting may not readily occur in *C. elegans* (Schwartz and Sternberg 2014; Xu 2015). Previous targeted approaches to identify potential off-target cutting by Cas9 did not identify bona fide off-target events (Chiu *et al.* 2013; Dickinson *et al.* 2013; Silva-García *et al.* 2019). Similarly, whole-genome sequencing-based approaches did not identify variants at predicted off-target sites and the overall rate of variant formation was not significantly higher than the spontaneous mutation rate (Paix *et al.* 2014; Waaijers and Boxem 2014; Au *et al.* 2018). Why have not previous approaches identified off-target cutting events in *C. elegans*? There are several contributing factors that might make identification of off-target cutting events difficult. We found that the efficiency of off-target cutting was much lower than on-target cutting (Figure 4), suggesting that off-target cutting events might be rare. Furthermore, off-target editing likely occurs in a heterozygous fashion, which can complicate detection in sequencing reactions since heterozygosity is rapidly lost in hermaphroditic organisms (Brenner 1974). Another factor could be the software used to design guide RNAs, many (or all) of which might not allow guides that carry single mismatches to other regions of the genome. Although we did not test whether multiple guide substitutions were more effective at blocking Cas9, previous studies have suggested that increasing the number of mismatches in the guide sequence leads to increased blocking of Cas9 (Jinek *et al.* 2012; Cong *et al.* 2013; Fu *et al.* 2013; Hsu *et al.* 2013; Mali *et al.* 2013; Pattanayak *et al.* 2013; Zhang *et al.* 2015). Thus, effective guide RNA design might essentially eliminate off-target cutting by Cas9. Our observation that off-target cutting can occur in *C. elegans* emphasizes the importance of careful guide design and backcrossing of genome-edited strains to remove potential unwanted mutations when off-target effects are suspected.

A temporal block to Cas9 activity appears to limit recutting of repaired DNA

Although we observe significantly reduced HDR editing rates when no blocking mutation was included in the ssODN repair template, the editing efficiency was high enough that we were able to reliably recover HDR-edited animals. Given the ability of Cas9 to target double-stranded repair templates, blocking conditions may remain critical for studies that use dsDNA repair templates. It is worth noting that many of the cases that might necessitate foregoing a blocking mutation, such as the editing of noncoding RNAs, would typically be small genomic changes that can be accomplished using ssODN repair templates.

The fact that we are able to recover HDR-edited animals without including a blocking mutation suggests that a temporal block to Cas9 activity exists in *C. elegans*, where the repaired region escapes repeated targeting by Cas9 (Figure 7E). What might lead to a temporal block to Cas9 activity? One possibility is that the reagents used for genome editing are not stable and/or targeted for degradation in the *C. elegans* germline, which would lead to reduced Cas9 activity over time. Consistent with this idea, RNP complexes are rapidly degraded (Kim *et al.* 2014; Liang *et al.* 2015; DeWitt *et al.* 2017; Prior *et al.* 2017; Farboud *et al.* 2019). Plasmid-expressed Cas9 may persist longer and might not result in the same temporal block that we observed for Cas9 RNP injection in this study. A second explanation for a temporal block might be that germ cells could become less receptive to Cas9 as they passage through the *C. elegans* germ line. Cas9 RNP complexes are injected into the syncytial maternal germline, where immature germ cells share a common cytoplasm and can all be targeted by a single injection (Evans 2006; Kadandale *et al.* 2008; Pazdernik and Schedl 2012; Hubbard and Schedl 2019). Many of the syncytial germ cells are in pachytene stage, during which time germ cells are receptive to homology directed repair pathways (Woglar and Jantsch 2014, McClendon *et al.* 2016). As germ cells mature, they could become less amenable to genome editing. Finally, it is also possible that genome editing reagents are diluted as they passage through the tubular-shaped maternal germline. This could explain the differences in editing efficiencies for maternal and paternal haplotypes, as the injection mix could become less available in the proximal germline. In any case, our findings suggest that Cas9 activity is attenuated over time, leading to a temporal block to Cas9 activity. This temporal block to Cas9 activity may then allow for effective HDR editing, even under conditions where Cas9 is not completely blocked. Additional work will be required to fully understand how a temporal block to Cas9 activity is established. It will also be interesting to see if a similar temporal block to Cas9 activity exists in other organisms, or if the unique germline architecture of *C. elegans* leads to reduced Cas9 activity over time.

Data availability

All strains and reagents used in this study are available upon request. The authors affirm that all necessary data to support the conclusions of this study are included within the manuscript.

Supplementary material is available at *GENETICS* online.

Acknowledgments

The authors thank current and former members of the Zinovyeva lab for valuable discussions and experimental assistance. They thank David Greenstein for providing helpful comments and suggestions. Some strains were provided by the CGC (*Caenorhabditis* Genetics Center), which is funded by the National Institutes of Health Office of Research Infrastructure Programs P40-OD010440.

Funding

This work was supported by a grant from the National Institute of General Medical Sciences (R35GM124828 to A.Y.Z.) and K-INBRE funds (P20 103GM418 to J.C.M. and J.T.S.).

Conflicts of interest

The authors declare that there is no conflict of interest.

Literature cited

Abbott AL, Alvarez-Saavedra E, Miska EA, Lau NC, Bartel DP, *et al.* 2005. The *let-7* MicroRNA family members *mir-48*, *mir-84*, and *mir-241* function together to regulate developmental timing in *Caenorhabditis elegans*. Dev Cell. 9:403–414. doi:10.1016/j.devcel.2005.07.009.

Alvarez-Saavedra E, Horvitz HR. 2010. Many families of *C. elegans* microRNAs are not essential for development or viability. Curr Biol. 20:367–373. doi:10.1016/j.cub.2009.12.051.

Arribere JA, Bell RT, Fu BX, Artiles KL, Hartman PS, *et al.* 2014. Efficient marker-free recovery of custom genetic modifications with CRISPR/Cas9 in *Caenorhabditis elegans*. Genetics. 198: 837–846. doi:10.1534/genetics.114.169730.

Au V, Li-Leger E, Raymant G, Flibotte S, Chen G, *et al.* 2018. CRISPR/Cas9 methodology for the generation of knockout deletions in *Caenorhabditis elegans*. G3 (Bethesda). 9:135–144. doi:10.1534/g3.118.200778.

Brenner S. 1974. The genetics of *Caenorhabditis elegans*. Genetics. 77: 71–94.

Ceccaldi R, Rondinelli B, D'Andrea AD. 2016. Repair pathway choices and consequences at the double-strand break. Trends Cell Biol. 26:52–64. doi:10.1016/j.tcb.2015.07.009.

Chang HHY, Pannunzio NR, Adachi N, Lieber MR. 2017. Non-homologous DNA end joining and alternative pathways to double-strand break repair. Nat Rev Mol Cell Biol. 18:495–506. doi:10.1038/nrm.2017.48.

Chen X, Feng X, Guang S. 2016. Targeted genome engineering in *Caenorhabditis elegans*. Cell Biosci. 6:60. doi:10.1186/s13578-016–0125-3.

Chiu H, Schwartz HT, Antoshechkin I, Sternberg PW. 2013. Transgene-free genome editing in *Caenorhabditis elegans* using CRISPR-Cas. Genetics. 195:1167–1171. doi:10.1534/genetics.113.155879.

Clejan I, Boerckel J, Ahmed S. 2006. Developmental modulation of nonhomologous end joining in *Caenorhabditis elegans*. Genetics. 173:1301–1317. doi:10.1534/genetics.106.058628.

Cong L, Ran FA, Cox D, Lin S, Barretto R, *et al.* 2013. Multiplex genome engineering using CRISPR/Cas systems. Science. 339:819–823. doi:10.1126/science.1231143.

Dejima K, Hori S, Iwata S, Suehiro Y, Yoshina S, *et al.* 2018. An aneuploidy-free and structurally defined balancer chromosome toolkit for *Caenorhabditis elegans*. Cell Rep. 22:232–241. doi:10.1016/j.celrep.2017.12.024.

Deltcheva E, Chylinski K, Sharma CM, Gonzales K, Chao Y, *et al.* 2011. CRISPR RNA maturation by trans-encoded small RNA and host factor RNase III. Nature. 471:602–607. doi:10.1038/nature09886.

DeWitt MA, Corn JE, Carroll D. 2017. Genome editing via delivery of Cas9 ribonucleoprotein. Methods. 121–122:9–15. doi:10.1016/j.ymeth.2017.04.003.

Dickinson DJ, Goldstein B. 2016. CRISPR-based methods for *Caenorhabditis elegans* genome engineering. Genetics. 202:885–901. doi:10.1534/genetics.115.182162.

Dickinson DJ, Ward JD, Reiner DJ, Goldstein B. 2013. Engineering the *Caenorhabditis elegans* genome using Cas9-triggered homologous recombination. Nat Methods. 10:1028–1034. doi:10.1038/nmeth.2641.

Dokshin GA, Ghanta KS, Piscopo KM, Mello CC. 2018. Robust genome editing with short single-stranded and long, partially single-stranded DNA donors in *Caenorhabditis elegans*. Genetics. 210:781–787. doi:10.1534/genetics.118.301532.

Doniach T. 1986. Activity of the sex-determining gene *tra-2* is modulated to allow spermatogenesis in the *C. elegans* hermaphrodite. Genetics. 114:53–76. doi:10.1093/genetics/114.1.53.

Duan Y, Choi S, Nelson C, Ambros V. 2020. Engineering essential genes with a "jump board" strategy using CRISPR/Cas9. MicroPubl Biol. 2020:10.17912/micropub.biology.000315. doi:10.17912/micropub.biology.000315.

Evans T. 2006. Transformation and microinjection. Wormbook. doi:10.1895/wormbook.1.108.1.

Farboud B. 2017. Targeted genome editing in *Caenorhabditis elegans* using CRISPR/Cas9. Wires Dev Biol. 6:e287. doi:10.1002/wdev.287.

Farboud B, Severson AF, Meyer BJ. 2019. Strategies for efficient genome editing using CRISPR-Cas9. Genetics. 211:431–457. doi:10.1534/genetics.118.301775.

Friedland AE, Tzur YB, Esvelt KM, Colaiácovo MP, Church GM, *et al.* 2013. Heritable genome editing in *C. elegans* via a CRISPR-Cas9 system. Nat Methods. 10:741–743. doi:10.1038/nmeth.2532.

Fu Y, Foden JA, Khayter C, Maeder ML, Reyon D, *et al.* 2013. High-frequency off-target mutagenesis induced by CRISPR-CAS nucleases in human cells. Nat Biotechnol. 31:822–826. doi:10.1038/nbt.2623.

Gallagher DN, Haber JE. 2021. Single-strand template repair: key insights to increase the efficiency of gene editing. Curr Genet. 67: 747–753. doi:10.1007/s00294-021–01186-z.

Gallagher DN, Pham N, Tsai AM, Janto AN, Choi J, *et al.* 2020. A Rad51-independent pathway promotes single-strand template repair in gene editing. PLoS Genet. 16:e1008689. doi:10.1371/journal.pgen.1008689.

Ghanta KS, Mello CC. 2020. Melting dsDNA donor molecules greatly improves precision genome editing in *Caenorhabditis elegans*. Genetics. 216:643–650. doi:10.1534/genetics.120.303564.

Haber JE. 2018. DNA repair: the search for homology. Bioessays. 40: 1700229. doi:10.1002/bies.201700229.

Han J, Huang J. 2020. DNA double-strand break repair pathway choice: the fork in the road. Genome Instab Dis. 1:10–19. doi:10.1007/s42764-019-00002-w.

Hodgkin JA, Brenner S. 1977. Mutations causing transformation of sexual phenotype in the nematode *Caenorhabditis elegans*. Genetics. 86:275–287.

Hsu PD, Scott DA, Weinstein JA, Ran FA, Konermann S, *et al.* 2013. DNA targeting specificity of RNA-guided Cas9 nucleases. Nat Biotechnol. 31:827–832. doi:10.1038/nbt.2647.

Hubbard EJA, Schedl T. 2019. Biology of the *Caenorhabditis elegans* germline stem cell system. Genetics. 213:1145–1188. doi:10.1534/genetics.119.300238.

Inui M, Miyado M, Igarashi M, Tamano M, Kubo A, *et al.* 2014. Rapid generation of mouse models with defined point mutations by the CRISPR/Cas9 system. Sci Rep. 4:5396. doi:10.1038/srep05396.

Iyer J, DeVaul N, Hansen T, Nebenfuehr B. 2018. Microinjection, methods and protocols. Methods Mol Biol. 1874:431–457. doi:10.1007/978-1-4939–8831-0_25.

Jiang F, Doudna JA. 2015. CRISPR–Cas9 structures and mechanisms. Annu Rev Biophys. 46:1–25. doi:10.1146/annurev-biophys-062215-010822.

Jinek M, Chylinski K, Fonfara I, Hauer M, Doudna JA, *et al.* 2012. A programmable dual-RNA–guided DNA endonuclease in adaptive bacterial immunity. Science. 337:816–821. doi:10.1126/science.1225829.

Kadandale P, Chatterjee I, Singson A. 2008. Microinjection, methods and applications. Methods Mol Biol. 518:123–133. doi:10.1007/978-1-59745-202-1_10.

Katic I, Großhans H. 2013. Targeted heritable mutation and gene conversion by Cas9-CRISPR in *Caenorhabditis elegans*. Genetics. 195:1173–1176. doi:10.1534/genetics.113.155754.

Katic I, Xu L, Ciosk R. 2015. CRISPR/Cas9 genome editing in *Caenorhabditis elegans*: evaluation of templates for homology-mediated repair and knock-Ins by homology-independent DNA repair. G3 (Bethesda). 5: 1649–1656. doi:10.1534/g3.115.019273.

Kim H, Colaiácovo MP. 2019. CRISPR-Cas9-guided genome engineering in *Caenorhabditis elegans*. Curr Protoc Mol Biol. 129:e106. doi:10.1002/cpmb.106.

Kim H, Ishidate T, Ghanta KS, Seth M, Conte D, *et al.* 2014. A Co-CRISPR strategy for efficient genome editing in *Caenorhabditis elegans*. Genetics. 197:1069–1080. doi:10.1534/genetics.114.166389.

Lewis BP, Shih I, Jones-Rhoades MW, Bartel DP, Burge CB. 2003. Prediction of mammalian MicroRNA Targets. Cell. 115:787–798. doi:10.1016/s0092-8674(03)01018-3.

Li J, Xu X. 2016. DNA double-strand break repair: a tale of pathway choices. Acta Biochim Biophys Sin (Shanghai). 48:641–646. doi:10.1093/abbs/gmw045.

Liang X, Potter J, Kumar S, Zou Y, Quintanilla R, *et al.* 2015. Rapid and highly efficient mammalian cell engineering via Cas9 protein transfection. J Biotechnol. 208:44–53. doi:10.1016/j.jbiotec.2015.04.024.

Lim LP, Lau NC, Weinstein EG, Abdelhakim A, Yekta S, *et al.* 2003. The microRNAs of *Caenorhabditis elegans*. Genes Dev. 17:991–1008. doi:10.1101/gad.1074403.

Liu M, Rehman S, Tang X, Gu K, Fan Q, *et al.* 2019. Methodologies for improving HDR efficiency. Front Genet. 9:691. doi:10.3389/fgene.2018.00691.

Ma D, Liu F. 2015. Genome editing and its applications in model organisms. Genom Proteom Bioinform. 13:336–344. doi:10.1016/j.gpb.2015.12.001.

Ma X, Wong AS-Y, Tam H-Y, Tsui SY-K, Chung DL-S, *et al.* 2018. *In vivo* genome editing thrives with diversified CRISPR technologies. Zool Res. 39:58–71. doi:10.24272/j.issn.2095–8137.2017.012.

Mali P, Aach J, Stranges PB, Esvelt KM, Moosburner M, *et al.* 2013. CAS9 transcriptional activators for target specificity screening and paired nickases for cooperative genome engineering. Nat Biotechnol. 31:833–838. doi:10.1038/nbt.2675.

Marraffini LA, Sontheimer EJ. 2010. Self versus non-self discrimination during CRISPR RNA-directed immunity. Nature. 463:568–571. doi:10.1038/nature08703.

McClendon TB, Sullivan MR, Bernstein KA, Yanowitz JL. 2016. Promotion of homologous recombination by SWS-1 in complex with RAD-51 paralogs in *Caenorhabditis elegans*. Genetics. 203:133–145. doi:10.1534/genetics.115.185827.

Miska EA, Alvarez-Saavedra E, Abbott AL, Lau NC, Hellman AB, *et al.* 2007. Most *Caenorhabditis elegans* microRNAs are individually not essential for development or viability. PLoS Genet. 3:e215. doi:10.1371/journal.pgen.0030215.

Mojica FJM, Díez-Villaseñor C, García-Martínez J, Almendros C. 2009. Short motif sequences determine the targets of the prokaryotic CRISPR defence system. Microbiology (Reading). 155:733–740. doi:10.1099/mic.0.023960-0.

Nance J, Frøkjær-Jensen C. 2019. The *Caenorhabditis elegans* transgenic toolbox. Genetics. 212:959–990. doi:10.1534/genetics.119.301506.

Okamoto S, Amaishi Y, Maki I, Enoki T, Mineno J. 2019. Highly efficient genome editing for single-base substitutions using optimized ssODNs with Cas9-RNPs. Sci Rep. 9:4811. doi:10.1038/s41598-019–41121-4.

Paix A, Folkmann A, Rasoloson D, Seydoux G. 2015. High efficiency, homology-directed genome editing in *Caenorhabditis elegans* using CRISPR-Cas9 ribonucleoprotein complexes. Genetics. 201:47–54. doi:10.1534/genetics.115.179382.

Paix A, Folkmann A, Seydoux G. 2017. Precision genome editing using CRISPR-Cas9 and linear repair templates in *C. elegans*. Methods. 121–122:86–93. doi:10.1016/j.ymeth.2017.03.023.

Paix A, Schmidt H, Seydoux G. 2016. Cas9-assisted recombineering in *C. elegans*: genome editing using *in vivo* assembly of linear DNAs. Nucleic Acids Res. 44:e128. doi:10.1093/nar/gkw502.

Paix A, Wang Y, Smith HE, Lee C-YS, Calidas D, *et al.* 2014. Scalable and versatile genome editing using linear DNAs with microhomology to Cas9 sites in *Caenorhabditis elegans*. Genetics. 198:1347–1356. doi:10.1534/genetics.114.170423.

Paquet D, Kwart D, Chen A, Sproul A, Jacob S, *et al.* 2016. Efficient introduction of specific homozygous and heterozygous mutations using CRISPR/Cas9. Nature. 533:125–129. doi:10.1038/nature17664.

Pattanayak V, Lin S, Guilinger JP, Ma E, Doudna JA, *et al.* 2013. High-throughput profiling of off-target DNA cleavage reveals RNA-programmed Cas9 nuclease specificity. Nat Biotechnol. 31:839–843. doi:10.1038/nbt.2673.

Pazdernik N, Schedl T. 2012. Germ cell development in *C. elegans*. Adv Exp Med Biol. 757:1–16. doi:10.1007/978-1-4614-4015-4_1.

Prior H, Jawad AK, MacConnachie L, Beg AA. 2017. Highly efficient, rapid and co-CRISPR-independent genome editing in *Caenorhabditis elegans*. G3 (Bethesda). 7:3693–3698. doi:10.1534/g3.117.300216.

Ranjha L, Howard SM, Cejka P. 2018. Main steps in DNA double-strand break repair: an introduction to homologous recombination and related processes. Chromosoma. 127:187–214. doi:10.1007/s00412-017–0658-1.

Reinhart BJ, Slack FJ, Basson M, Pasquinelli AE, Bettinger JC, *et al.* 2000. The 21-nucleotide *let-7* RNA regulates developmental timing in *Caenorhabditis elegans*. Nature. 403:901–906. doi:10.1038/35002607.

Richardson CD, Kazane KR, Feng SJ, Zelin E, Bray NL, *et al.* 2018. CRISPR–Cas9 genome editing in human cells occurs via the Fanconi anemia pathway. Nat Genet. 50:1132–1139. doi:10.1038/s41588-018–0174-0.

Sashital DG, Wiedenheft B, Doudna JA. 2012. Mechanism of Foreign DNA selection in a bacterial adaptive immune system. Mol Cell. 46:606–615. doi:10.1016/j.molcel.2012.03.020.

Schwartz HT, Sternberg PW. 2014. Chapter twenty transgene-free genome editing by germline injection of CRISPR/Cas RNA. Methods Enzymol. 546:441–457. doi:10.1016/b978-0–12-801185-0.00021-0.

Scully R, Panday A, Elango R, Willis NA. 2019. DNA double-strand break repair-pathway choice in somatic mammalian cells. Nat Rev Mol Cell Biol. 20:698–714. doi:10.1038/s41580-019–0152-0.

Shrock E, Güell M. 2017. Chapter six CRISPR in animals and animal models. Prog Mol Biol Transl. 152:95–114. doi:10.1016/bs.pmbts.2017.07.010.

Silva-García CG, Lanjuin A, Heintz C, Dutta S, Clark NM, *et al.* 2019. Single-copy knock-in loci for defined gene expression in *Caenorhabditis elegans*. G3 (Bethesda). 9:2195–2198. doi:10.1534/g3.119.400314.

Sun Y, McCorvie TJ, Yates LA, Zhang X. 2020. Structural basis of homologous recombination. Cell Mol Life Sci. 77:3–18. doi:10.1007/s00018-019–03365-1.

Vella MC, Choi E-Y, Lin S-Y, Reinert K, Slack FJ. 2004. The *C. elegans* microRNA *let-7* binds to imperfect *let-7* complementary sites from the *lin-41* 3′UTR. Genes Dev. 18:132–137. doi:10.1101/gad.1165404.

Waaijers S, Boxem M. 2014. Engineering the *Caenorhabditis elegans* genome with CRISPR/Cas9. Methods. 68:381–388. doi:10.1016/j.ymeth.2014.03.024.

Wang H, Park H, Liu J, Sternberg PW. 2018. An efficient genome editing strategy to generate putative null mutants in *Caenorhabditis elegans* using CRISPR/Cas9. G3 (Bethesda). 8:3607–3616. doi:10.1534/g3.118.200662.

Ward JD. 2015. Rapid and precise engineering of the *Caenorhabditis elegans* genome with lethal mutation co-conversion and inactivation of NHEJ repair. Genetics. 199:363–377. doi:10.1534/genetics.114.172361.

Woglar A, Jantsch V. 2014. Chromosome movement in meiosis I prophase of *Caenorhabditis elegans*. Chromosoma. 123:15–24. doi:10.1007/s00412-013–0436-7.

Xu S. 2015. The application of CRISPR-Cas9 genome editing in *Caenorhabditis elegans*. J Genet Genomics. 42:413–421. doi: 10.1016/j.jgg.2015.06.005.

Yang H, Ren S, Yu S, Pan H, Li T, *et al.* 2020. Methods favoring homology-directed repair choice in response to CRISPR/Cas9 induced-double strand breaks. Int J Mol Sci. 21:6461. doi: 10.3390/ijms21186461.

Yoshimi K, Kunihiro Y, Kaneko T, Nagahora H, Voigt B, *et al.* 2016. ssODN-mediated knock-in with CRISPR-Cas for large genomic regions in zygotes. Nat Commun. 7:10431. doi:10.1038/ncomms 10431.

Zhang X-H, Tee LY, Wang X-G, Huang Q-S, Yang S-H. 2015. Off-target effects in CRISPR/Cas9-mediated genome engineering. Mol Ther Nucleic Acids. 4:e264. doi:10.1038/mtna.2015.37.

Zhao B, Rothenberg E, Ramsden DA, Lieber MR. 2020. The molecular basis and disease relevance of non-homologous DNA end joining. Nat Rev Mol Cell Biol. 21:765–781. doi:10.1038/s41580-020–00297-8.

Zhao P, Zhang Z, Ke H, Yue Y, Xue D. 2014. Oligonucleotide-based targeted gene editing in *C. elegans* via the CRISPR/Cas9 system. Cell Res. 24:247–250. doi:10.1038/cr.2014.9.

Communicating editor: H. Buelow